Annual Report 2023

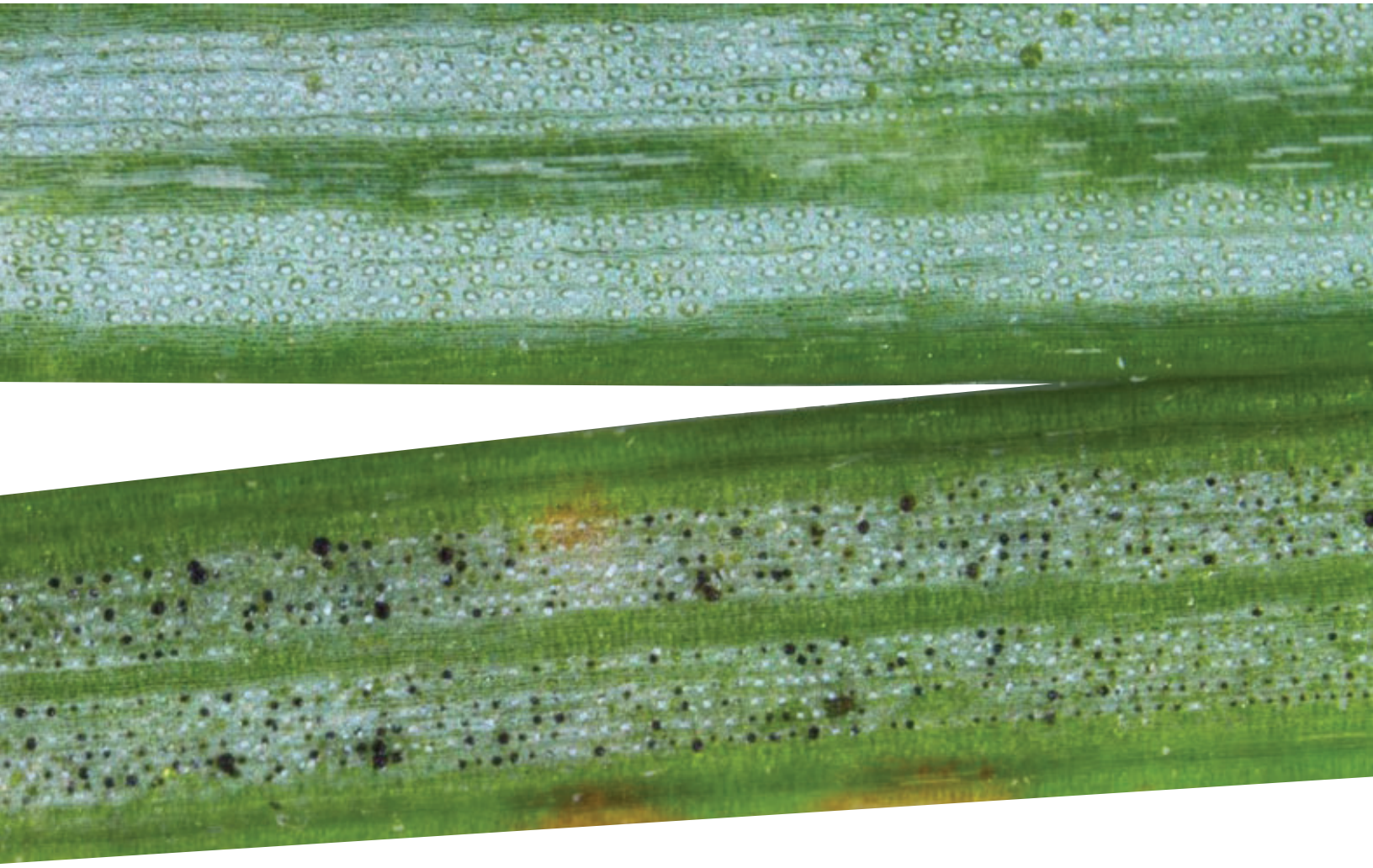

Oregon State University
College of Forestry

Swiss Needle Cast Cooperative

Oregon State University | College of Forestry

Starker Forests, Inc.

Members of the Swiss Needle Cast Cooperative

Cascade Timber Consulting

Greenwood Resources, Inc. Lewis & Clark Tree Farms, LLC

Oregon Department of Forestry

Rayonier, Inc.

Starker Forests

USDA Forest Service

Weyerhaeuser Corporation

Swiss Needle Cast Cooperative Staff

Dave Shaw – Director and Associate Professor of Forest Health

Adam Carson – Associate Director and Faculty Research Assistant

SNCC Income Sources and Expenditures: 2023

Income	
Membership dues	*84,000*
Oregon State Legislature	*95,000*
Carry-over	*279,370*
Total 2023 Income	**$458,370**
Expenditures	
Salaries and wages	*106,583*
Travel	*13,175*
Operating expenses	*15,536*
Materials and Supplies	*10,224*
Indirect Costs (@17.5%)	*5,111*
Total 2023 Expenditures	**$145,518**
Balance	**$312,582**

SNCC Background and Organization

A major challenge to intensive management of Douglas fir in Oregon and Washington is the current Swiss needle cast (SNC) epidemic. Efforts to understand the epidemiology, symptoms, and growth losses from SNC have highlighted gaps in our knowledge of basic Douglas-fir physiology, growth, and silviculture. The original mission of the Swiss Needle Cast Cooperative (SNCC), formed in 1997, was broadened in 2004 to include research aiming to ensure that Douglas-fir remains a productive component of the Coast Range forests. The SNCC is located in the Department of Forest Engineering, Resources and Management within the College of Forestry at Oregon State University. The Membership is comprised of private, state, and federal organizations. Private membership dues are set at a fixed rate. An annual report, project reports, and newsletters are distributed to members each year. Our objective is to carry out projects in cooperation with members on their land holdings.

SNCC Mission

To conduct research on enhancing Douglas-fir productivity and forest health in the presence of Swiss needle cast and other diseases in coastal forests of Oregon and Washington.

SNCC Objectives

(1) Understand the epidemiology of Swiss needle cast and the basic biology of the causal fungus, *Nothophaeocryptopus gaeumannii*.

(2) Design silvicultural treatments and regimes to maximize Douglas-fir productivity and ameliorate disease problems in the Coast Range of Oregon and Washington.

(3) Understand the growth, structure, and morphology of Douglas-fir trees and stands as a foundation for enhancing productivity and detecting and combating various diseases of Douglas-fir in the Coast Range of Oregon and Washington.

Department of Forest Engineering, Resources and Management
Oregon State University
216 Peavy Forest Science Complex
Corvallis, Oregon 97331

P 541-737-4952
F 541-737-4316
ferm.forestry.oregonstate.edu

3/16/2024

To: Swiss Needle Cast Membership
From: David Shaw, Past Director 2023

Greeting Membership,

Things are really happening these days, and the SNCC continues to make progress on research and monitoring of SNC, collaborate with everyone working on SNC, and continually improve our knowledge of SNC epidemiology in Oregon Forests and beyond. Our research and monitoring plot network in the Oregon Coast Range, and our monitoring plots in the western Cascades, coupled with the Aerial Detection survey, gives members great insight into what is happening with the SNC epidemic today. We are especially excited about our collaboration with the Center for Intensive Plantation Forest Silviculture, in using our data to improve growth and yield modeling.

As you may know, I've stepped down as Director of the SNCC and am retiring from OSU. Jared LeBoldus is the new Director of the SNCC, and Adam Carson continues as the FRA for the SNCC. I believe the SNCC is set up to move into a new era of research with fresh perspectives and solution driven research. Jared and Adam are very accomplished forest pathologists, and bring a wealth of knowledge and leadership to the SNCC.

I'd like to thank the cooperative members for your support of research at Oregon State University. The cooperatives are a unique feature of the College of Forestry. The connection of foresters and research faculty working together to solve forestry problems is a model for the world I think.

Finally, I'd like to say that I am honored to have served as Director of the SNCC and feel like the SNCC was something that sustained my optimism about how academia can collaborate with people who manage the land. Of course, the paradigm of my colleagues at OSU Forestry and Natural Resources Extension Service is exactly that: academia is here to help people!

Sincerely,

David C. Shaw
2023 Director, SNCC

Ten-Year Remeasurement of the Swiss Needle Cast Cooperative Research and Monitoring Plots, Installation of a New Network of Monitoring Transects, and Spore Trapping for *Nothophaeocryptopus gaeumannii*

2023 Research Activities of the Swiss Needle Cast Cooperative

Adam Carson[1], Gabriela Ritóková[2], Dave Shaw[1], Jared LeBoldus[1,3]

[1] SNCC, Forest Engineering, Resources, and Management, Oregon State University, [2]Oregon Department of Forestry, [3]Department of Botany and Plant Pathology, Oregon State University

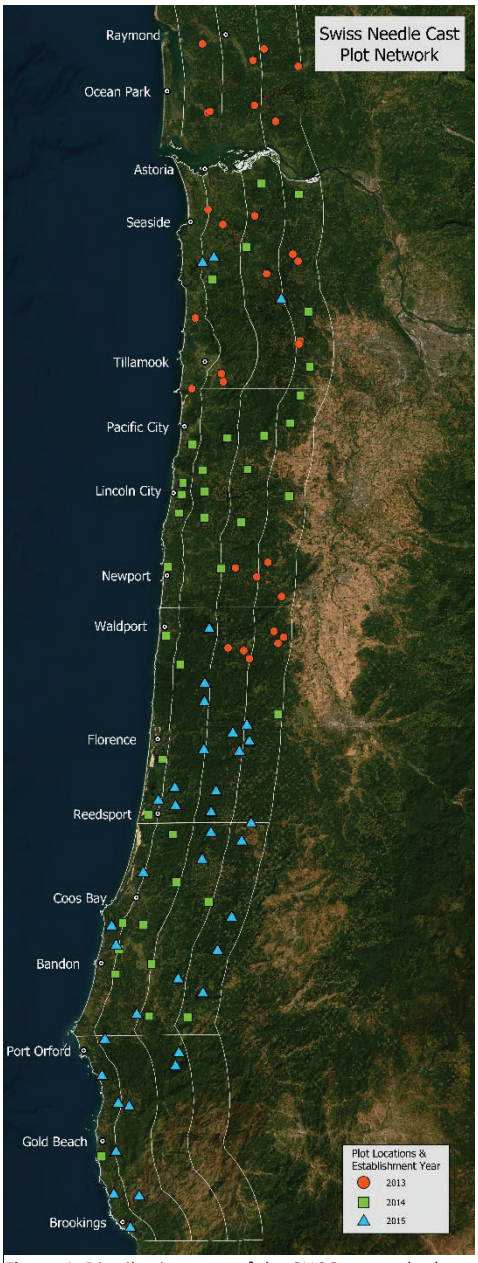

Figure 1. Distribution map of the SNCC research plot network.

Remeasuring the Research and Monitoring Plot Network

The research and monitoring plot network (RPN), established by the Swiss Needle Cast Cooperative (SNCC), consists of 106 plots installed in Douglas-fir plantations distributed along the coast range from Oregon and southwest Washington (Fig. 1). Installation of the network began in 2013 and took 3 years to complete. Four of the research plots have since been lost due to precommercial thinning and wildfire. This network provides information on the geographic distribution and disease severity of Swiss needle cast (SNC) across the landscape, as well as growth and yield impacts to Douglas-fir. The first five-year remeasurement of the remaining 102 plots was completed in 2020. From this first re-measurement, cubic volume growth loss of 30-35% was estimated in heavily infected SNC stands with low needle retention (Mainwaring et al. 2020). This is a reduced estimate from the previous 50% growth loss calculated in 2011 (Maguire et al. 2011). Furthermore, initial assessments of foliage retention within the RPN found that disease severity increased and foliage retention decreased with latitude (Ritóková et al. 2021). Analyses from the initial and first remeasurement of the RPN can be found in the 2020 SNCC Annual Report.

The second five-year remeasurement (ten-years post establishment) of the RPN is currently underway and will conclude in 2026. The measurement of the first 30 plots (those established in 2013) were completed in the fall of 2023, and foliage samples will be collected from these plots to assess needle retention and disease severity in the spring of 2024. The first third of the RPN plots are distributed within the four northernmost latitudinal sampling zones and are included in all four longitudinal zones (Fig. 1). Analysis of the data from the first 30 plots, and their implications on cubic volume growth, are discussed on page 10 of this report (Mainwaring et al. 2024).

A New Network for Monitoring SNC

In addition to the RPN, the SNCC monitors SNC disease conditions within the foothills of the Cascade mountains using a network of monitoring transects. Thirty-four transects were installed in 10-to-15-year-old Douglas-fir stands in the spring and summer of 2023 (Fig. 2). Each selected stand contains a single 100-meter transect with five sample points located at 20-meter intervals. At each sample point, the nearest co-dominant or dominant Douglas-fir on each side of the transect are selected for a total of 10 trees per stand. Diameter at breast height, foliage retention, and disease severity is collected for each sampled tree. Each transect is representative of the stand in which it was established.

This new network replaces a retired network of monitoring transects installed in 2017 by the SNCC. These transects will be surveyed annually with the aim of evaluating SNC conditions using an index rating system for disease severity (Fig. 3) and foliage retention (Fig. 4). The results from the original network indicated that the disease is present over time despite observed improvements in foliage retention and reduced disease severity overall.

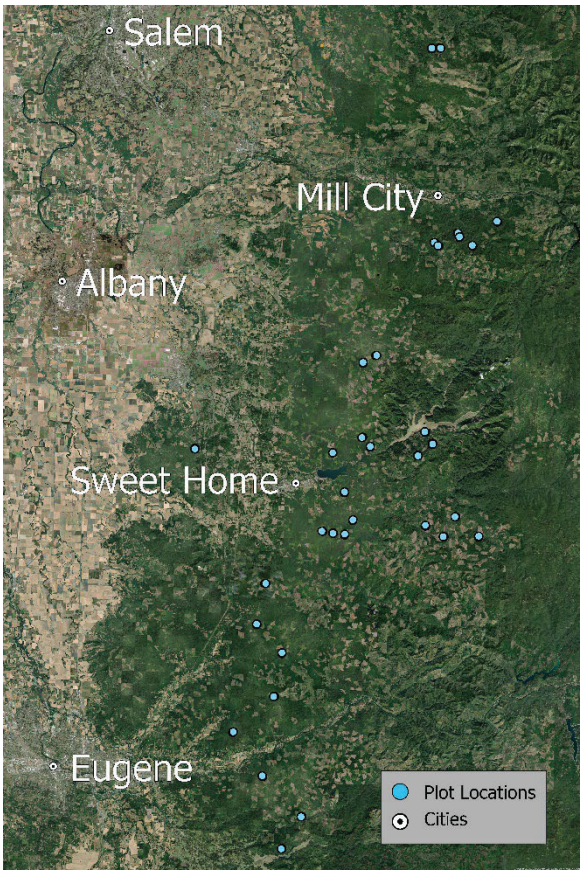

Figure 2. Distribution map of the new network of Cascade foothills SNC monitoring transects.

The first full assessment of the updated transect network will occur in the spring of 2024. However, preliminary results from the subset of stands sampled in 2023 indicate that disease severity ranged from 1.2 to 2.1 (light to moderate), and foliage retention varied between 2.0 and 3.3 years. Across all stands surveyed, the mean foliage retention was 2.83, and the mean disease severity was 1.73. The correlation between disease severity and foliage retention in these stands was weak (Fig. 5). However, there was a strong positive correlation betweeen foliage retention and elevation, and all stands above 1900 feet exhibited foliage retention greater than 2.8 years (Fig. 6).

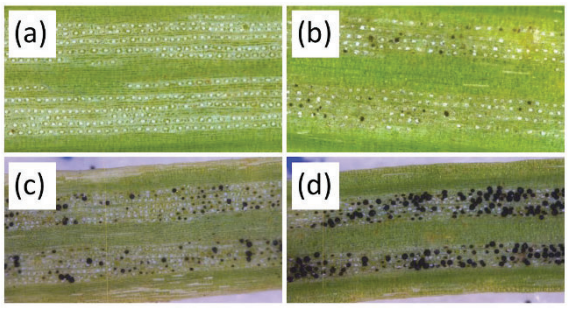

Figure 3. Disease severity index rating for cascade monitoring transects. (a) No pseudothecia present = 0; (b) light stomatal occlusion, up to 20% = 1; (c) moderate occlusion, between 20-50% = 2; (d) heavy occlusion, above 50% = 3.

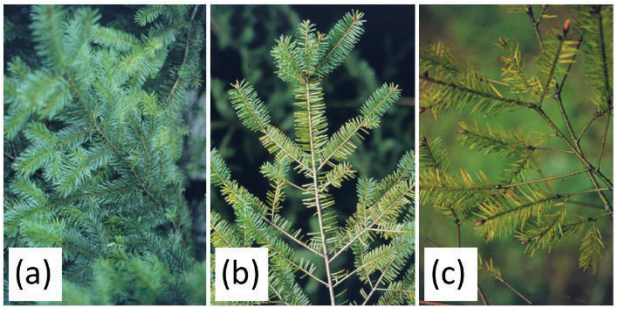

Figure 4. Examples of foliage retention ratings on 4-year lateral branches. (a) full needle retention across all 4 cohorts = 4; (b) near full retention on 1st & 2nd cohorts, partial retention on 3rd & 4th cohorts = 2.4; (c) partial retention on 1st cohort only = 0.9.

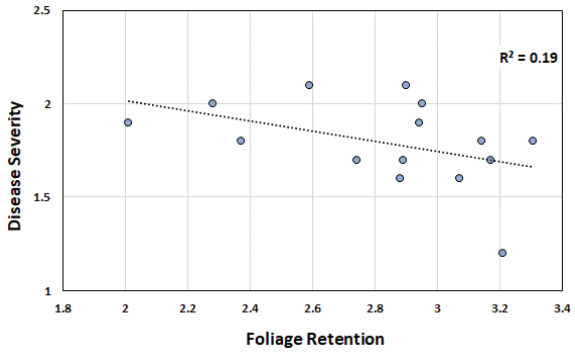

Figure 5. Disease severity and foliage observed at the plot level.

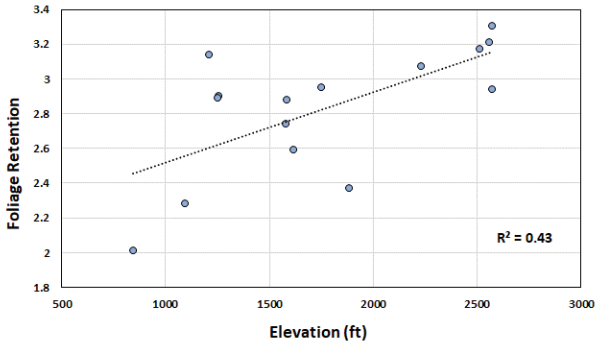

Figure 6. Foliage retention and elevation observed at the plot level.

Spore Trapping for *Nothophaeocryptopus gaeumannii*

Little is known about the spatial and seasonal spread of spores of *N.* gaeumannii. As a result, many questions about SNC epidemiology remain unanswered. In 2023 the SNCC piloted a spore-trapping study in collaboration with Dr. Miloň Dvořák of Mendel University in the Czech Republic and Gabriela Ritóková from the Oregon Department of Forestry. The goal of this project was to refine methodologies developed from a previous proof of concept study conducted by the SNCC in 2021 to capture and detect airborne spores of *N. gaeumannii*. The results from the 2023 study are intended to aid in the development of future research projects aimed at comparing the dispersal patterns of inoculum and SNC in the landscape.

The initial construction of the in-house SNCC rotating arm impaction spore traps was based on a design by Walter F. Mahaffee (USDA-ARS) and the description of Dvořák et al. (2017). The instruments were then modified in 2023 to optimize efficiency for capturing the targeted particle size of *N. gaeumannii* spores (7.86 µm diameter) at a sampling rate of 74.49 L per hour. Each trap utilizes a 12 V electrical motor that rotates at 4,450 rotations per minute with two horizontal rotary arms connected to vertical impaction rods made from 20-gauge yellow brass wire (3.7 x 0.08 cm) affixed with double-sided tape (Fig. 7). Spores are captured on one side of the tape on each rod for a total impaction area of 5.92 mm^2 per trap. Each spore trap is mounted on a free-standing wooden frame and is powered by two 6 V batteries connected in series (Fig. 8).

In June of 2023, three re-designed rotating arm impaction spore traps were deployed in a heavily SNC-infected coastal Douglas-fir stand located near Pacific City, Oregon. The traps ran for a 24-hour sampling period after which time the samples were collected and transported to Oregon State University for processing. Detection of *N. gaeumannii* spores from the collected samples follows the quantitative polymerase chain reaction (qPCR) protocol described by Mireia Gómez-Gallego et al. (2019) using genomic DNA extracted from the spore trap samples. While the results of the 2023 study are still pending, the detection protocol was tested in 2021 and was successful at detecting *N. gaeumannii* from collected spores trap samples. Additionally, the measurements following the recalibration of the spore traps indicate that the design of these instruments is now well-suited for capturing the targeted particle size of *N. gaeumannii* spores. The final processing of the 2023 spore trap samples is expected to be completed in the spring of 2024.

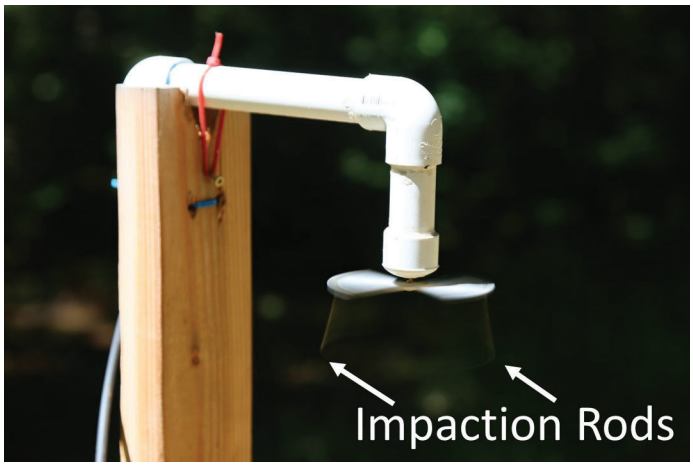

Figure 7. Running spore trap with double-sided tape affixed to the impaction rods. Photo by Miloň Dvořák.

Figure 8. Running spore traps and batteries mounted on wooden frames. Photo by Miloň Dvořák.

Literature Cited

Dvořák, M., Janoš, P., Botella, L., Rotková, G., & Zas, R. (2017). Spore dispersal patterns of *Fusarium circinatum* on an infested Monterey pine forest in North-Western Spain. *Forests*, *8*(11), 432.

Gómez-Gallego, M., LeBoldus, J. M., Bader, M. K. F., Hansen, E., Donaldson, L., & Williams, N. M. (2019). Contrasting the pathogen loads in co-existing populations of *Phytophthora pluvialis* and *Nothophaeocryptopus gaeumannii* in Douglas fir plantations in New Zealand and the Pacific Northwest United States. *Phytopathology, 109*(11), 1908-1921.

Maguire, D. A., Mainwaring, D. B., & Kanaskie, A. (2011). Ten-year growth and mortality in young Douglas-fir stands experiencing a range in Swiss needle cast severity. *Canadian Journal of Forest Research*, *41*(10), 2064-2076.

Mainwaring, D., Maguire, D., Ritóková, G., & Shaw, D. Volume growth losses within Swiss Needle Cast Infected Douglas-fir plantations, 2013-2020. *Swiss Needle Cast Cooperative*, *1*, 24.

Ritóková, G., Mainwaring, D. B., Shaw, D. C., & Lan, Y. H. (2021). Douglas-fir foliage retention dynamics across a gradient of Swiss needle cast in coastal Oregon and Washington. *Canadian Journal of Forest Research*, *51*(4), 573-582.

Swiss needle cast research plot network: second remeasurement of group 1 plots

Doug Mainwaring, Gabriela Ritóková, Dave Shaw, and Adam Carson

Abstract

The second five-year remeasurement of the first third of the SNCC research plot network (RPN) has been completed (30 plots). The negative effect of SNC on cubic volume growth during the second 5-year period was compared to that on the same plots during the first five-year period. The negative effect of SNC due to diminished foliage retention was found to be ~23% greater during the second period for the lowest estimated initial foliage retention (1.2 years). The greater estimated negative effect of foliage retention during period two is similar to that estimated for the 1998-2008 GIS plots. Some of this difference may be due to positive changes in foliage retention between period 1 and period 2. The potential for changes in foliage retention during the five-year growth periods of the current plot network have the potential of affecting estimated growth losses, and should be accounted for in future analyses.

Introduction

The RPN was initiated in 2013 to address two major objectives: 1) to monitor Swiss needle cast (SNC) symptoms and tree growth in 10-25-yr-old Douglas-fir plantations throughout the Oregon Coast Range and southwest Washington; and 2) to provide an improved estimate of growth losses associated with a given initial level of SNC. Volume growth losses were estimated to average 23% for the target population in 1996, with losses reaching 50% in the most severely impacted stands. Four subsequent remeasurements through 2008 confirmed these estimates (Maguire et al. 2011). In contrast, during the five-year period of the RPN's first measurement period, estimated cubic volume growth losses were a maximum of ~35% at a foliage retention of 1.0 years.

The objectives of this report are: 1) to quantify the most recent 5-yr growth responses relative to initial SNC severity; and 2) to compare this 5-yr growth responses to those estimated for the same plots from 2013-2018.

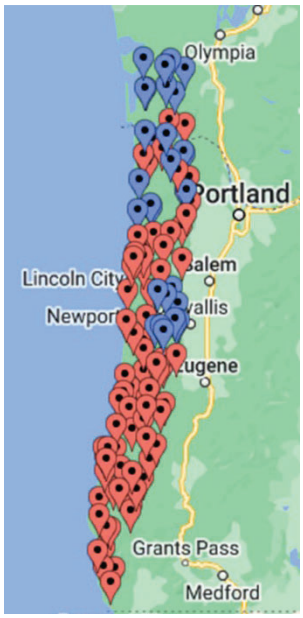

Figure 1 Location of the SNCC RPN; Blue symbols show location of the group 1 plots analyzed in this report.

Methods

Study sites

Establishment of the RPN began in the Fall of 2013, and ultimately included 106 plots installed over three years. These plots were established in 10-25 year old Douglas-fir plantations (>80% BA in Douglas-fir) that had not been treated in the last five years, and were distributed from the Oregon-California border to SW Washington, and from the coastline to 35 miles inland

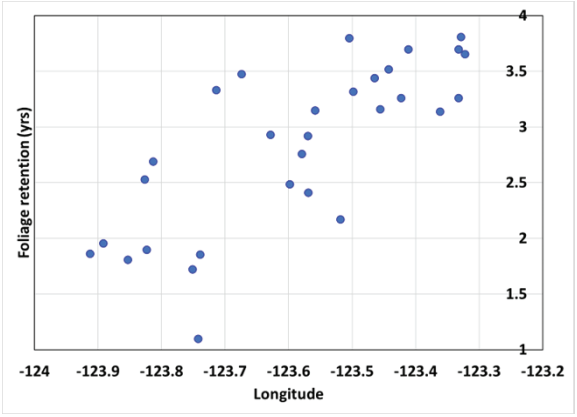

Figure 2 Distribution of foliage retention by longitude.

(Ritóková et al. 2017). These plots and their measurement protocols are identical to the original Growth Impact Plots (Maguire et al. 2011).

In the spring following establishment, and again following the second remeasurement, foliage retention (nearest 0.1 year) was estimated from laterals within the middle crown third of five dominant trees on the plot. In young stands with highly visible crowns, this could usually be done visually from the ground; for older stands, estimation required climbing. Data summaries of the plot network can be found in a previous SNC annual report (Ritóková et al. 2017).

The second remeasurement of the first thirty plots of the network took place in the fall of 2023 (fig. 1). These plots were generally in the northern half of the network, and tended to have a greater proportion of plots with lower levels of SNC than subsequent remeasurement groups (fig. 2).

Statistical analysis

The equation for estimating the stand level cubic volume for the entire plot network was:

$$[1] \quad CFV\_PAI = a_1 \cdot (BA_{df}^{a2}) \cdot \exp(a_3 \cdot BA_{ndf}) \cdot SI_{adj}^{a4} \cdot (1-\exp(a_5+a_6 \cdot FR^3))$$

With CFV_PAI being the five-year periodic annual cubic volume increment (volumes estimated using CIPSANON), BA_{df} was stand level Douglas-fir basal area, BA_{ndf} was stand level basal area of all other species, SI_{adj} was site index adjusted for foliage retention (Mainwaring et al. 2020), and FR was initial foliage retention at the start of the period. For the smaller 30 plot subset, a_3 and a_4 were insignificant predictors, resulting in the reduced equation [2], fit separately to each period:

$$[2] \quad CFV\_PAI = a_1 \cdot (BA_{df}^{a2}) \cdot (1-\exp(a_5+a_6 \cdot FR^3))$$

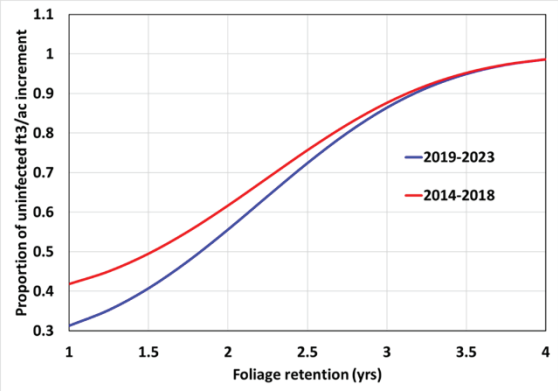

Figure 4 Estimated growth losses from separate period fits to equation [2].

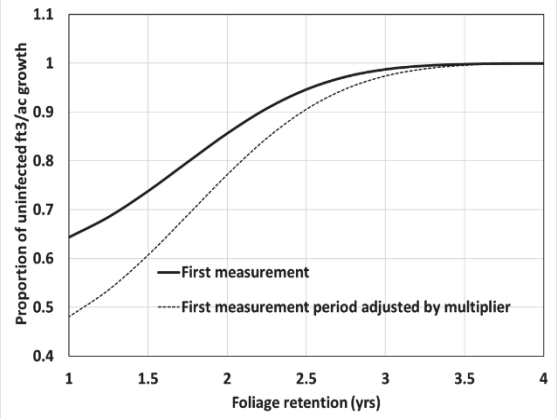

Figure 4 Ratio of the foliage retention effect during period 2 to the foliage retention effect during period 1.

Results and Discussion

The fit to the data resulted in separate estimates of a_5 and a_6 (equation [2]). Expressed graphically, period 2 cubic growth losses for a given foliage retention were estimated to be greater (fig. 3). The absolute loss estimate (1.0 - Y-axis value) should be ignored due to the limited size of the dataset and the over-representation of uninfected plots. A relative comparison of the two periods (full dataset first period growth loss adjusted by relative losses shown in fig. 3) is a more appropriate comparison, and this indicates that growth losses at the lowest foliage retentions estimated at the start of period two were about ~23% greater than that estimated during period one (fig. 4). This greater growth loss

also implies a comparable growth loss in period two as estimated for the GIS plots during the growth periods between 1998 and 2008 (~50%).

Figure 5 indicates that during the five years between 2013 and 2018, the average foliage retention on the group 1 plots increased on the most infected plots, by an average of ~0.3 years. This means that while growth loss estimates during period one were based on the initial value, improvements in foliage retention on infected plots during the period would have presumably improved growth, diminishing the losses for a given initial foliage retention. We will not know the comparable (end of period) foliage retention on these plots until the spring of 2024. Stasis or negative changes in foliage retention during this second period would result in the opposite effect than seen for the first period. A proper analysis of this data will need to account for changes in foliage retention during the five-year periods, with the recognition that some significant changes during the five-year period could go unaccounted for due to the period length.

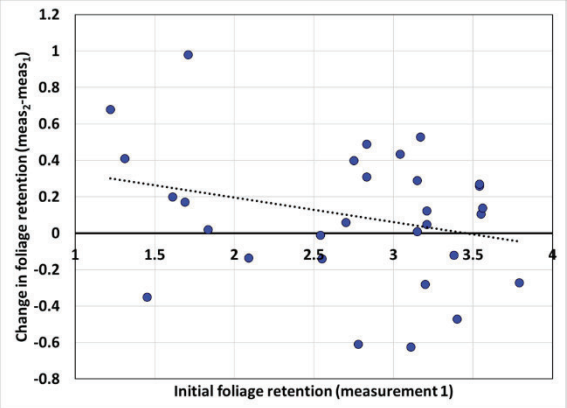

Figure 5 Change in initial foliage retentions between periods two and one for the thirty plots of group one.

Literature Cited

Bruce, D., 1981. Consistent height-growth and growth-rate estimates for remeasured plots. For. Sci. 27:711-725.

Maguire, D.A., Mainwaring, D.B. and Kanaskie, A., 2011. Ten-year growth and mortality in young Douglas-fir stands experiencing a range in Swiss needle cast severity. Can. J. For. Res. 41:2064-2076.

Mainwaring. D., Maguire, D., Ritóková, G. and Shaw, D. 2020. Volume growth losses within Swiss needle cast infected Douglas-fir plantations, 2013-2020. P. 24-30 in Swiss Needle Cast Cooperative annual report, Shaw, D., and Ritokova, G. (eds.). College of Forestry, Oregon State Univ., Corvallis, OR.

Ritóková, G., Shaw, D., Maguire, D., Mainwaring, D., Browning, J., Gourley, M., Filip, G., Kanaskie, A., and Marshall, B. 2017. Swiss Needle Cast Cooperative Research and Monitoring Plot Network in Coastal Oregon, Southwestern Washington, and Oregon Cascade Foothills. P. 7-13 in Swiss Needle Cast Cooperative annual report, Shaw, D., and Ritokova, G. (eds.). College of Forestry, Oregon State Univ., Corvallis, OR.

Climatic adaptation in the genetic lineages of the Swiss Needle Cast pathogen

Nicolas Feau[1] and Richard C. Hamelin[2]

[1]Pacific Forestry Centre, Canadian Forest Service/Natural Resources Canada

[2]Department of Forest and Conservation Sciences, University of British Columbia, Vancouver, BC, Canada, VT6 1Z4

In recent decades, changing environmental conditions have coincided with periodic epidemics of the Swiss Needle Cast disease (SNC) of Douglas-fir in the coastal forests of the Pacific Northwest (PNW) that started on the Oregon coast and that are now spreading to higher latitudes in British-Columbia, Canada[1]. Using whole genome sequencing and population genomics approaches, we identified genetic differences in *N. gaeumannii*, the fungus responsible of the SNC disease, that could constitute a source of variability in climate response and disease severity. Two highly divergent genetic lineages of *N. gaeumannii* (lineage 1 and 2), with different levels of suitability to climates, have been identified, increasing concerns that the fungus may rapidly adapt to new environments. We found that lineage 1 can be further subdivided in lineage 1c and 1i. Lineages 1c and 2 are sympatric on needles of the coastal variety of Douglas-fir, *Pseudotsuga* menziesii var. *menziesii* while lineage 1i is primarily associated with the Rocky Mountain variety of this tree, *P. menziesii* var. *glauca*. Modeling of the demographic and evolutionary history based on genetic variation found among ~200 SNC genomes indicated that lineage 1c and 1i diverged from a common ancestor about 20,000 years ago. This coincides with the divergence between the respective host of each of these lineages, the coastal Douglas-fir and the Rocky Mountain Douglas-fir, after the last glacial maximum. The absence of genomic barriers to sexual reproduction as-well-as a strong conservation of the mating-type genes among lineages invalidated the original hypothesis of complete reproductive isolation between the three lineages. Instead, strong evidence of gene-flow was detected between lineage 1c and 1i, with hybridization events likely happening on trees located in the

hybrid zone of coastal and Rocky Mountain Douglas-fir. Similarly, introgressive hybridization going from lineage 2 to lineage 1c was detected, suggesting that genes with adaptive functions are likely transferred between these two sympatric lineages. Using a genotype-by-environment association approach we found that a significant part of the genetic variation between the lineage 1c and 2 can be explained by few climatic variables. Lineage 2 is adapted to cooler temperatures in cold months, while lineage 1c contains genomic signatures of adaptation to lower precipitations during summer months and the larger range of temperatures observed inland. These predictions were corroborated by phenotyping data and distribution modeling that showed that lineage 1c had a higher adaptive plasticity to temperatures than lineage 2 and that the current environmental tolerance range of lineage 1c should keep exceeding that of lineage 2.

Swiss Needle Cast Cooperative BC Update 2023 – David.Rusch@gov.bc.ca

BC has 43 “Oregon style” SNC permanent sample plots established over a period of 3 years starting in 2017 (Table 1). Fifteen of the plots have weather stations. Five-year re-measurements have been conducted on all of the plots but foliar sampling still needs to be completed on 7 of the plots established in 2019.

Table 1. Number of plots by bio-geoclimatic subzone, plot establishment year and location. CWHxm = very dry coastal western hemlock, CWHdm = Coastal Western Hemlock dry maritime, CWHvm=Coastal Western Hemlock very moist maritime.

Plot Establishment Year	Vancouver Island	Sunshine Coast	Lower Fraser Valley
2017			13 CWHdm
2018	18 CWHxm	3 CWHxm, 2 CWHdm	
2019			7 CWHvm

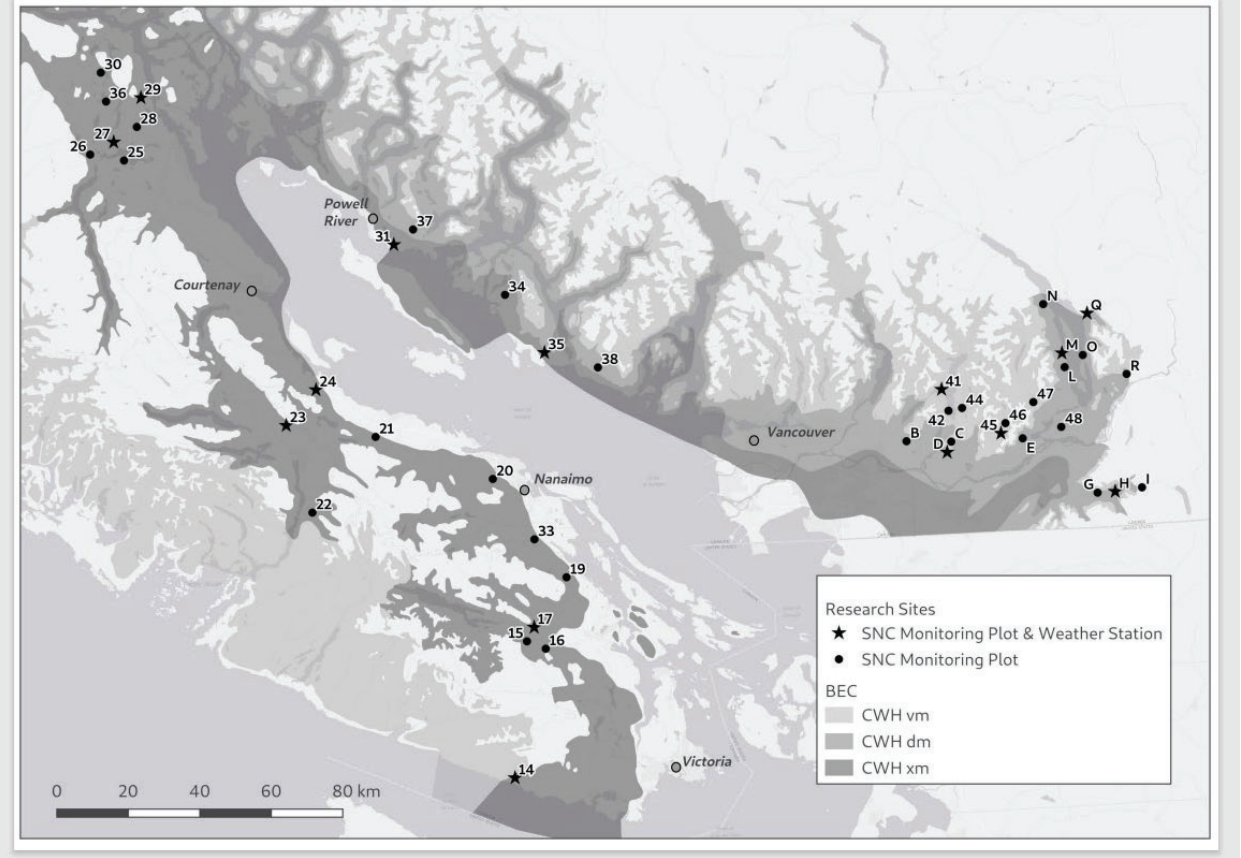

Figure 1. Map of BC Swiss Needle Cast plots

Needle retention for all plots is shown in Figure 2. For the bottom third 5-year re-measurement, needle retention on the side branch located closest to the bole was compared to needle retention from the end of the main branch axis. On average needle retention close to the bole was one year greater than needle retention at the end of the branch. Average disease incidence as measured by % needles with pseudothecia, decreased from the bottom crown third to the top crown third for most of the plots but

Dynamics of the phyllosphere fungal microbiome in Douglas-fir needles associated with *Nothophaeocryptopus gaeumannii* in coastal Oregon, USA

Yung-Hsiang Lan[1] and Jared LeBoldus[1,2]

Department of Botany and Plant Pathology, Oregon State University

Department of Forest Engineering, Resources, and Management, Oregon State University

Introduction

The foliar fungal community is important for host resistance to diseases (Saikkonen et al 1998). Foliar microbiomes can also be related to plant physiological traits such as stomatal conductance (Arnold and Engelbrecht 2007) and affect host responses to abiotic stress. *Nothophaeocryptopus gaeumannii* is the most abundant member of Douglas-fir needles (Gervers et al 2022). It also causes a common disease known as Swiss Needle Cast (SNC) on the Oregon coast. The disease occurs when pseudothecia emerge in the spring blocking the stomata, affecting gas exchange, and reducing tree growth. This growth loss results in more than $200 million in productivity form Douglas-fir forests per year (Maguire et al 2002). The main objective of this study is to understand if phylloshpere fungal communities relate to *N. gaeumannii* occlusion and SNC abundance. Our research goals are to: (1) characterize the foliar microbiome community of mature Douglas-fir trees at the Elliott State Forest; (2) evaluate the incidence and severity of SNC across the Elliot State Forest; and (3) correlate the foliar microbiome community with SNC incidence and local microclimate.

Field methods

In fall 2022, nine mature Douglas-fir trees were selected to represent the environment and stand conditions at the Eliot State Forest (Fig. 1). Within the selected trees, four are located in foggy areas and five are located in non-foggy areas. For each tree, we first measured the length from the tree-top to the lowest contiguous (vertical distance < 2m) branch. This distance was considered the canopy depth. Canopy depth is divided into five equal vertical segments, within each segment we flagged four aspects (N, E, S, and W) for sampling (Fig.2). In November 2022, we collected 2.5-year-old needles for foliar microbiome analysis (Fig. 3), and in June 2023 we collected 3-year-old needles, the same cohort we sampled previously, for foliar microbiome analysis. We also measured SNC incidence and severity in the spring on 3-year-old needles.

Samples were temporarily stored at 5ºC after collection. Microbiome samples were transferred and stored at -20ºC before processing. SNC samples were stored at 5ºC prior to incidence and severity rating.

To address the environmental differences among canopies at foggy and non-foggy plots, we selected one tree from the foggy area and one tree from non-foggy area, temperature and humidity sensors (HOBO Onset MX2301A) were placed at each sample location (5 heights × 4 aspects × 2 trees).

Lab methods and data analysis

Microbiomes

Foliar samples were lyophilized for 24 hours and stored at -80 ºC. DNA samples were extracted by using OPS 96 well SYNERGY plant extraction kits. The ITS2 region was first amplified using the 5.85-Fun and ITS4-Fun primers, a 3-6 bp length heterogeneity spacer, and then illumina adaptor sequences (Gervers et al 2022). The amplified samples were normalized and purified by Just-A-Plate (Charm Biotech) and QIAquick PCR purification kits. The completed library was sent to the Center for Quantitative Life Science at OSU for genome sequencing.

Sequencing data was trimmed and paired using R (v.4.2.2, R Core Team 2022), and the following packages: DADA2 (v1.25.2, Callahan et al., 2016), ggplot2 (Wickham 2016), phyloseq (McMurdie and Holmes, 2013), and vegan (Oksanen et al 2022) were used to identify the fungal species in the sequences. The UNITE general FASTA release was used as fungal taxonomy matrix (https://unite.ut.ee/repository.php). Using non-metric multidimensional scaling (NMDS) to foliar fungal community diversity was explored. Permutational Multivariate Analysis of Variance (PERMANOVA) was used to test which environmental variables best explained the fungal community.

SNC evaluation

For each sample, we first evaluated the needle retention of 4 years of needles, then randomly selected fifty 3-year-old needles, taped them to an index card, and stored at -20ºC. Initially, we recorded the incidence of pseudothecia, defined as the number of needles with pseudothecia

occlusions from the 50 needles (Fig. 4). For a subset of 10 needles with pseudothecia present, we conducted density counts to evaluate infection severity. We applied a generalized linear mixed effects model in R to test if foliage retention or SNC incidence was different among plots, canopy heights, and branch directions.

Preliminary results

Phyllosphere microbiome

The preliminary suggested that the fungal phyllosphere communities were significantly different between foggy and non-foggy plots (p=0.0001), and among the different sampling heights (p=0.002). The fungal communities in the phyllosphere varied with time of collection (p=0.005). However, the communities did not differ among sampling directions (p=0.38) (Fig. 5). *N. gaeumannii* was present in most samples (Fig. 6), other needle pathogens, such as *Rhabdocline* spp., and some lichen associated species, like *Cliostomum griffithi* and *Scoliciosporum* spp*,* were also detected in the phyllosphere (Fig 6).

Foliage retention

Foliage retention was significantly different between foggy and non-foggy plots (p=0.0009) (Fig. 7). Needle retention in the foggy plots was 0.62 years less than non-foggy plots. Also, south facing needles had a foliar retention 0.35 years greater than north facing needles (p=0.005). However, needle retention was not statistically different among canopy heights.

SNC incidence

SNC incidence was significantly different between foggy and non-foggy plots (p=0.02). SNC incidence in the foggy plots was 52% greater than non-foggy plots. SNC incidence at the lowest canopy was 29% higher than SNC incidence at the top of the canopy (p=0.007). SNC incidence was not statistically different among the four directions.

Pseudothecia density and SNC severity index

Pseudothecia density was significantly different between foggy and non-foggy plots (p<0.001); however, SNC severity index was not different (p=0.60). Neither pseudothecia or SNC severity index were different at canopy heights and directions. Although SNC incidence was greater in

foggy plots, there were fewer pseudothecia on each infected needle. In non-foggy plots, the infected needles had higher portion of stomatal occlusion but fewer needles were infected.

Microclimate

The temperature was more dynamic at higher canopy positions. The dew point temperature was higher in foggy sites than in unfoggy site, suggesting the foggy site has a greater chance of fog or frost in the canopy.

References

Arnold, A.E., Engelbrecht, B.M.J., 2007. Fungal endophytes nearly double minimum leaf conductance in seedlings of a neotropical tree species. J. Trop. Ecol. 23, 369-372.

Callahan, B.J., McMurdie, P.J., Rosen, M.J., Han, A.W., Johnson, A.J.A., Holmes, S.P., 2016. DADA2: High-resolution sample inference from Illumina amplicon data. Nature Methods, 13(7), 581–583.

Gervers, K.A., Thomas, D.C., Roy, B.A., Spatafora, J.W., Busby, P.E., 2022. Crown closure affects endophytic leaf mycobiome compositional dynamics over time in *Pseudotsuga menziezii* var. *menziesii*. Fungal Ecol. 57-58, 101155.

Lan, Y.-H., Shaw, D.C., Beedlow, P.A., Lee, E.H., Waschmann, R.S., 2019. Severity of Swiss needle cast in young and mature Douglas-fir forests in western Oregon, USA. For. Eco. Manag. 442, 79-95.

Maguire, D.A., Kanaskie, A., Voelker, W., Johnson, G., 2002. Growth of young Douglas-fir plantations across a gradient in Swiss Needle Cast severity. West. J. Appl. Forestry 17(2), 86-95.

McMurdie, P.J., Holmes, S., 2013. Phyloseq: An R package for reproducible interactive analysis and graphics of microbiome census data. PLoS ONE 8(4):e61217.

Oksanen, J., Simpson, G., Blanchet, F., Kindt, R., Legendre, P., Minchin, P., O'Hara, R., Solymos, P., Stevens, M., Szoecs, E., Wagner, H., Barbour, M., Bedward, M., Bolker, B., Borcard, D., Carvalho, G., Chirico, M., De Caceres, M., Durand, S., Evangelista, H., FitzJohn, R., Friendly, M., Furneaux, B., Hannigan, G., Hill, M., Lahti, L., McGlinn, D., Ouellette, M., Ribeiro Cunha, E., Smith, T., Stier, A., Ter Braak, C., Weedon, J., 2022. Vegan: Community Ecology Package_. R package version 2.6-4, https://CRAN.R-project.org/package=vegan

R Core Team (2022). R: A language and environment for statistical computing. R Foundation for Statistical Computing, Vienna, Austria. https://www.R-project.org/

Saikkonen, K., Faeth, S.H., Helander, M., Sulliva, T.J., 1998. Fungal endophytes: a continuum of interactions with host plants. Annu. Rev. Ecol. Syst. 29, 319-343.

Wickham, H., 2016. ggplot2: Elegant Graphics for Data Analysis. Springer-Verlag New York.

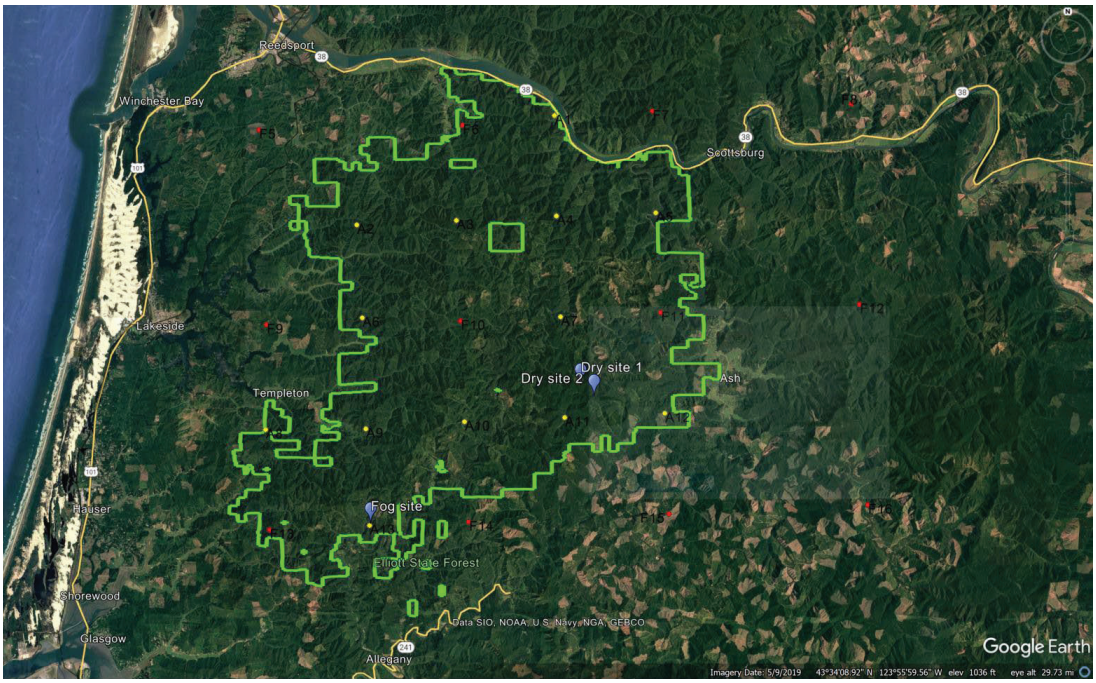

Figure 1. Map of study area. The green line is the boundary of Elliott State Forest. Blue dots are the tree locations.

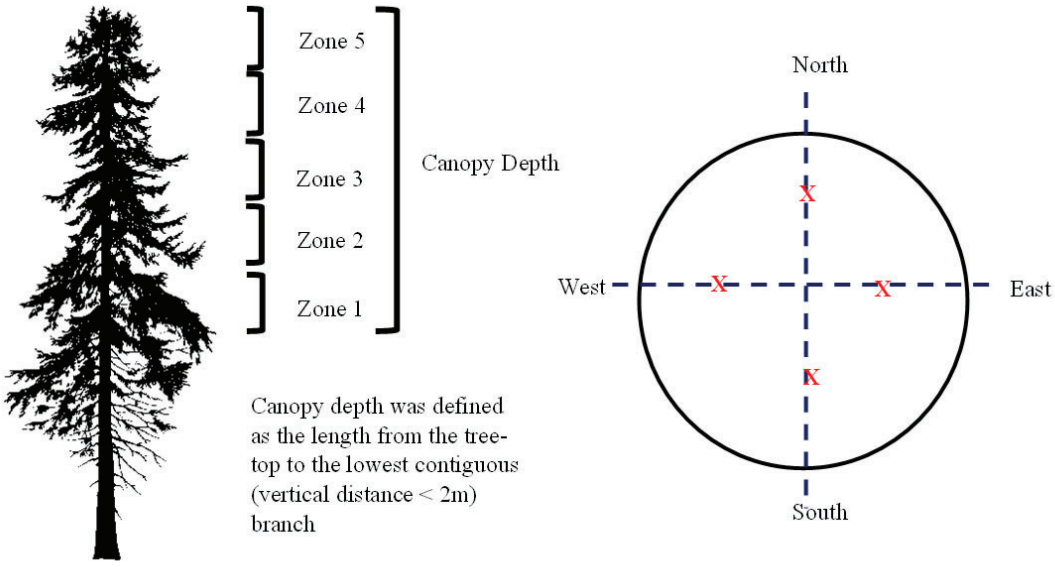

Figure 2. Sampling layout for monitoring old growth canopy microbiomes (left). Samples are collected separately from 4 aspects within each zone (right).

Figure 3. Tree climbers taking microbiome samples on the tree. (Photos by Brian French)

Figure 4. Picture of pseudothecia. The white dots on the needle are stomata, the black dots in the stomata are pseudothecia. (Photo by Yung-Hsiang Lan)

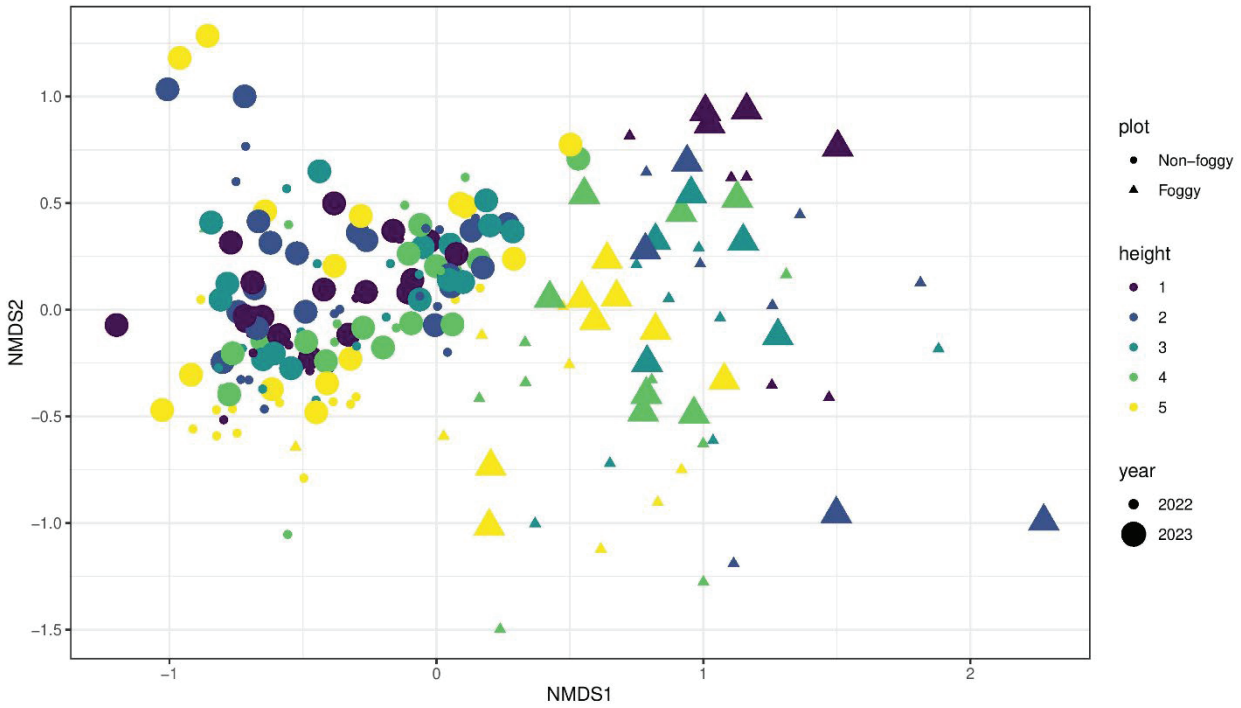

Figure 5. Non-metric multidimensional scaling (NMDS) results of all ASVs. Height 1 to 5 represent the canopy height beginning at the bottom to the top of trees.

(A)

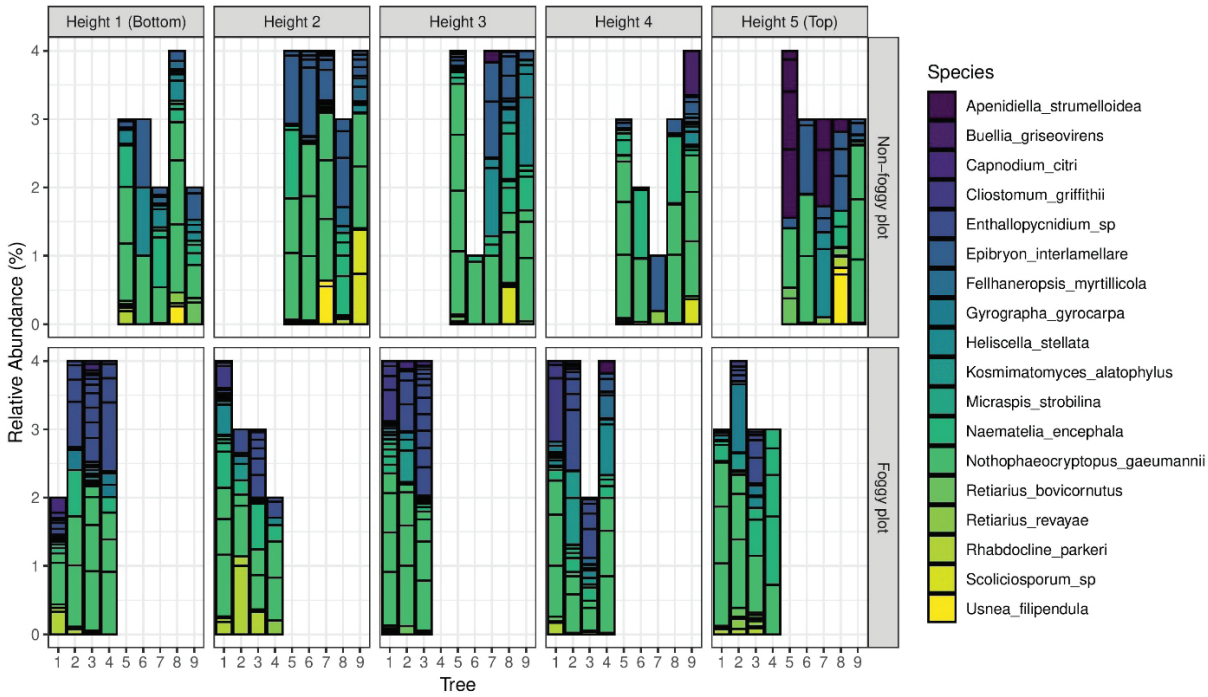

(B)

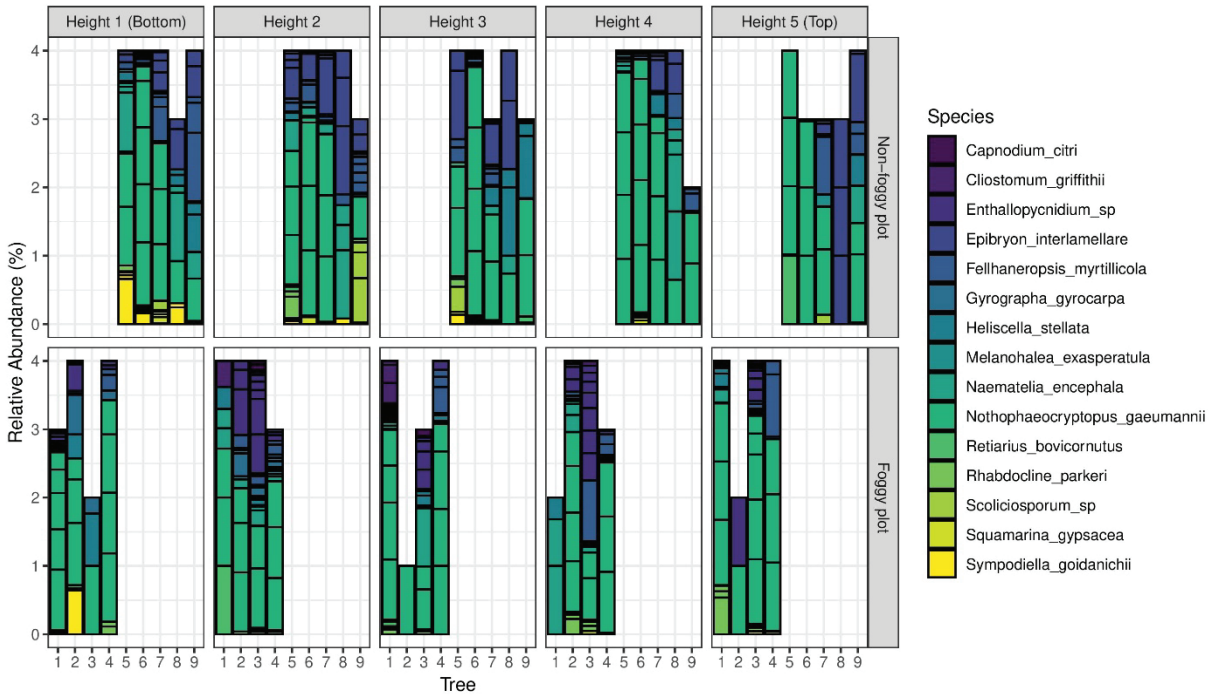

Figure 6. The relative abundance of the known species of the 100 most abundant ASVs (amplicon sequence variants). The top figure (A) was from 2022 collection, and the bottom figure (B) was from 2023 collection. Height 1 to 5 represent the canopy height beginning at the bottom to the top of trees.

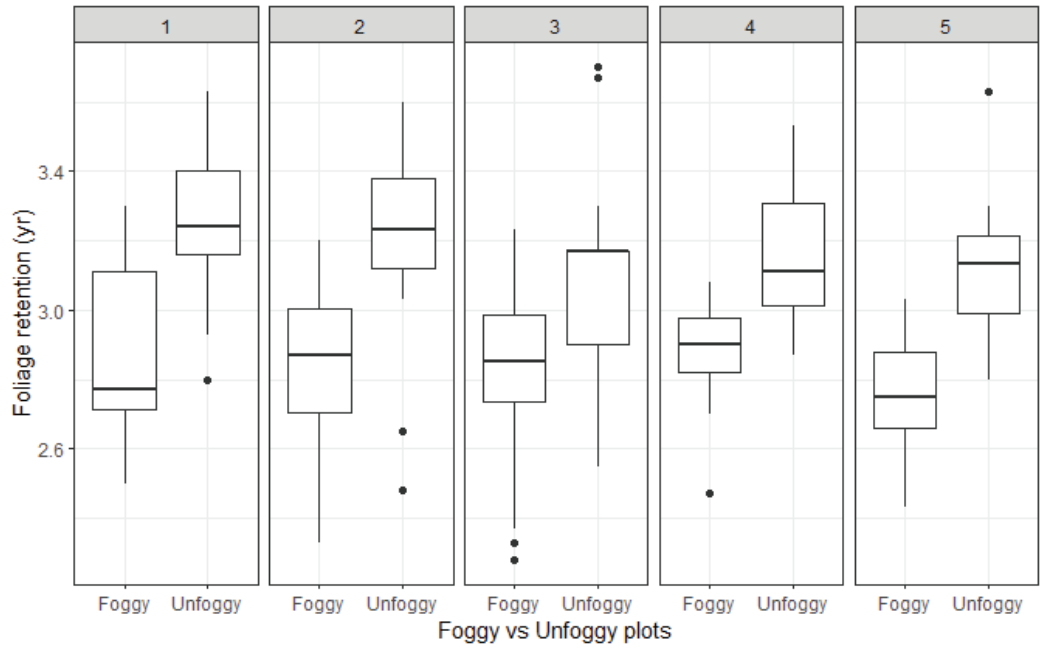

Figure 7. Foliage retention. Numbers 1 to 5 represent the canopy height beginning at the bottom to the top of trees.

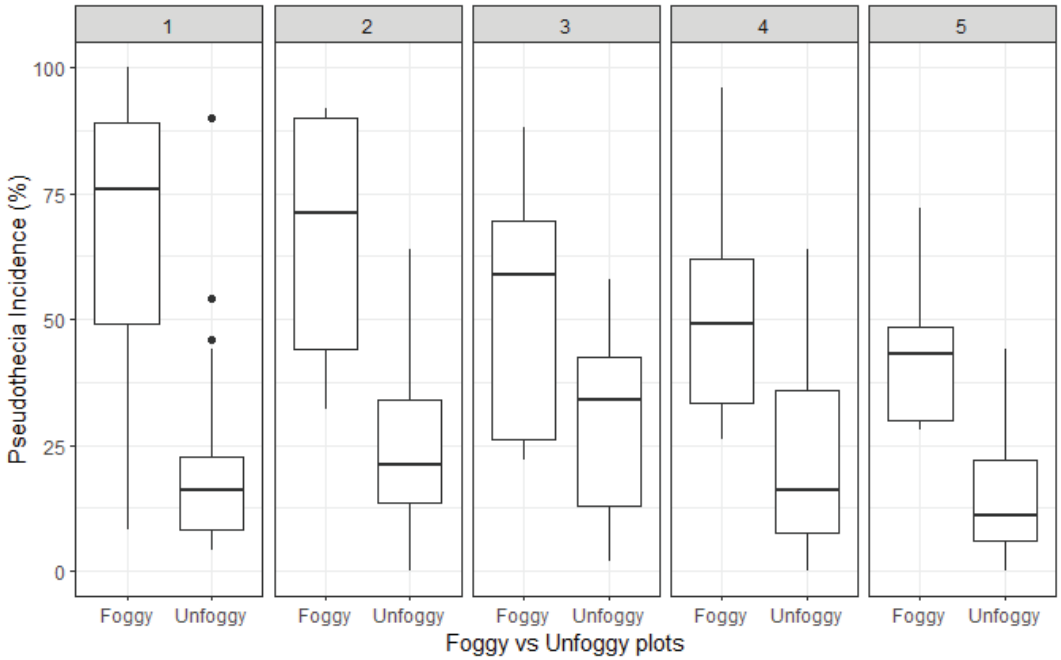

Figure 8. SNC incidence. Numbers 1 to 5 represent the canopy height beginning at the bottom to the top of trees.

(A)

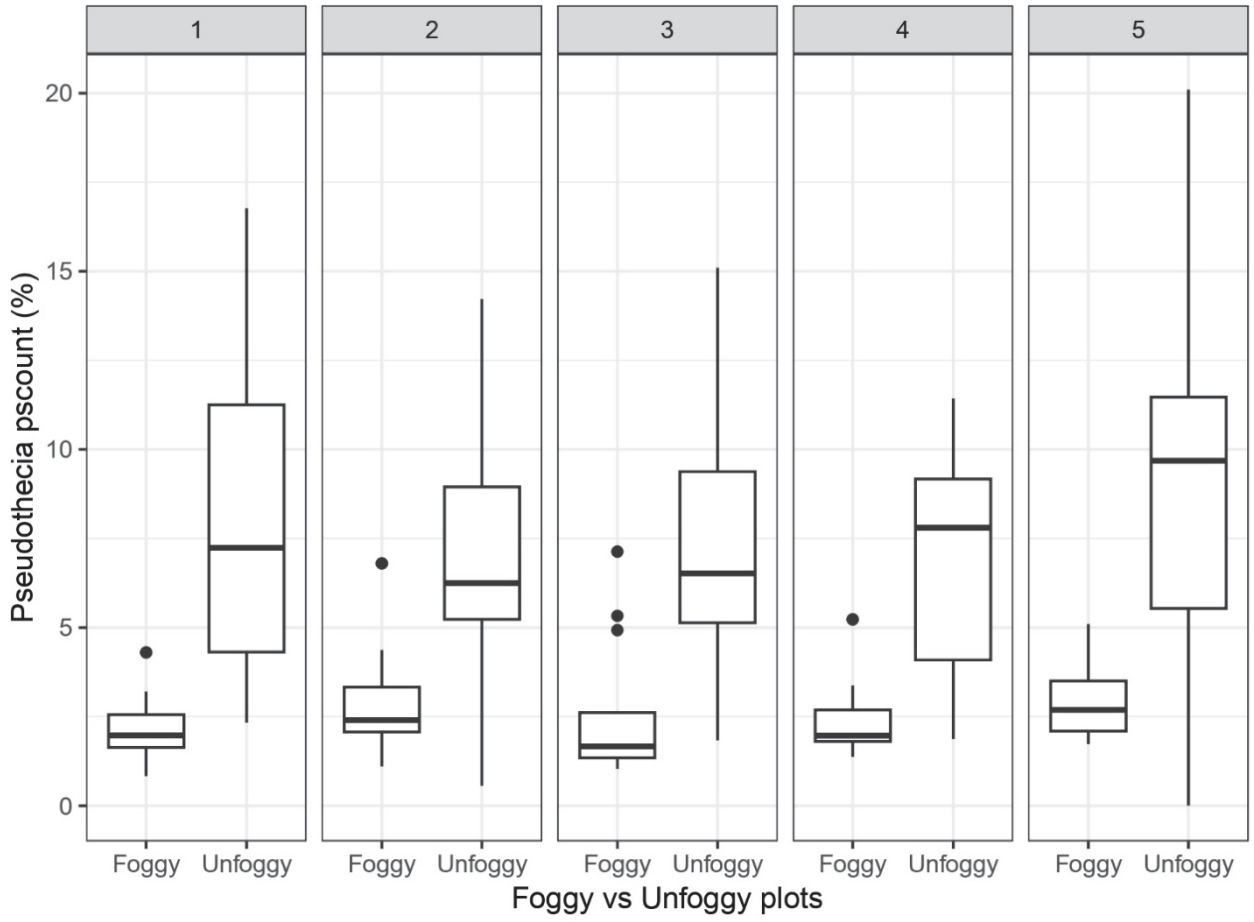
1
2
3
4
5
Pseudothecia pscount (%)
20
15
10
5
0
Foggy
Unfoggy
Foggy vs Unfoggy plots

(B)

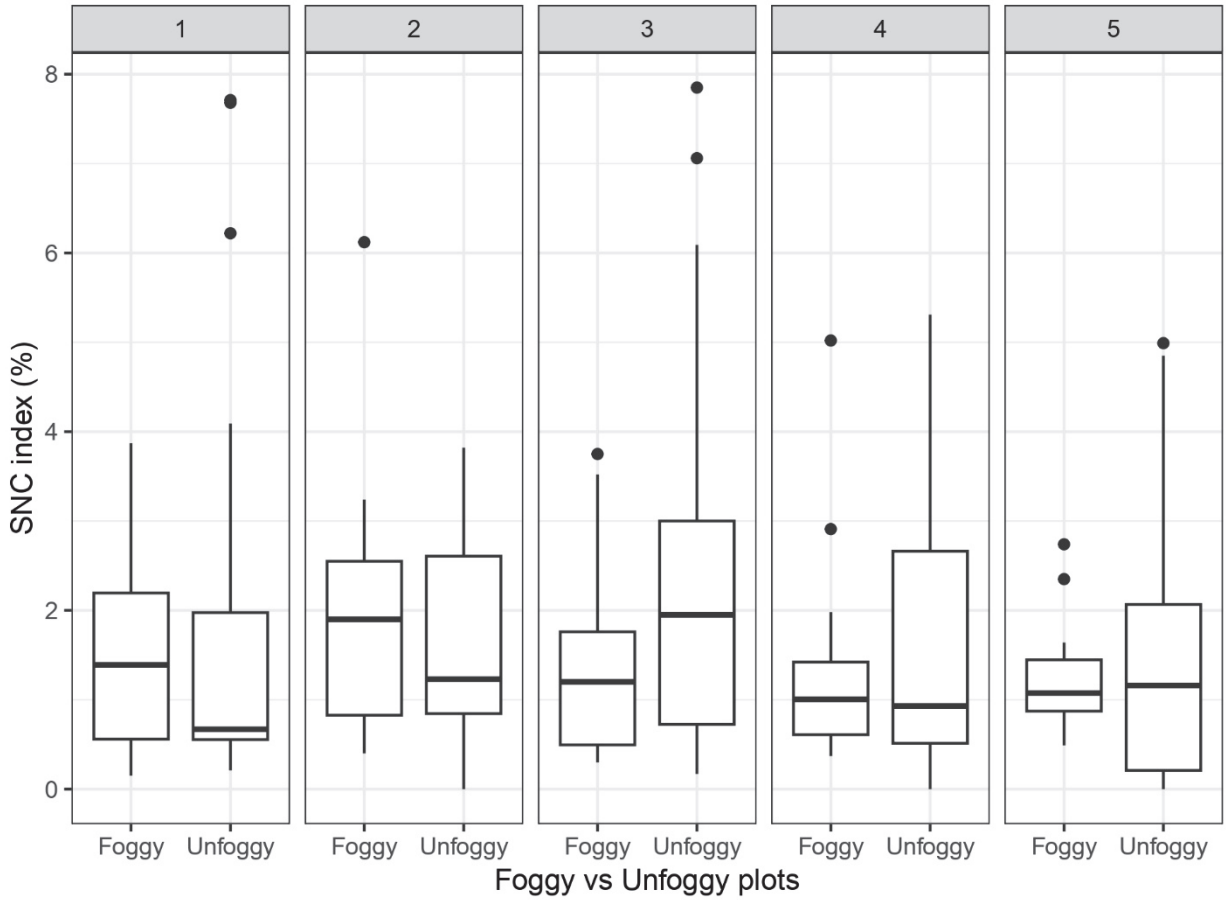

Figure 9. Pseudothecia density (A) and SNC severity index (B). Numbers 1 to 5 represent the canopy height beginning at the bottom to the top of trees.

(A)

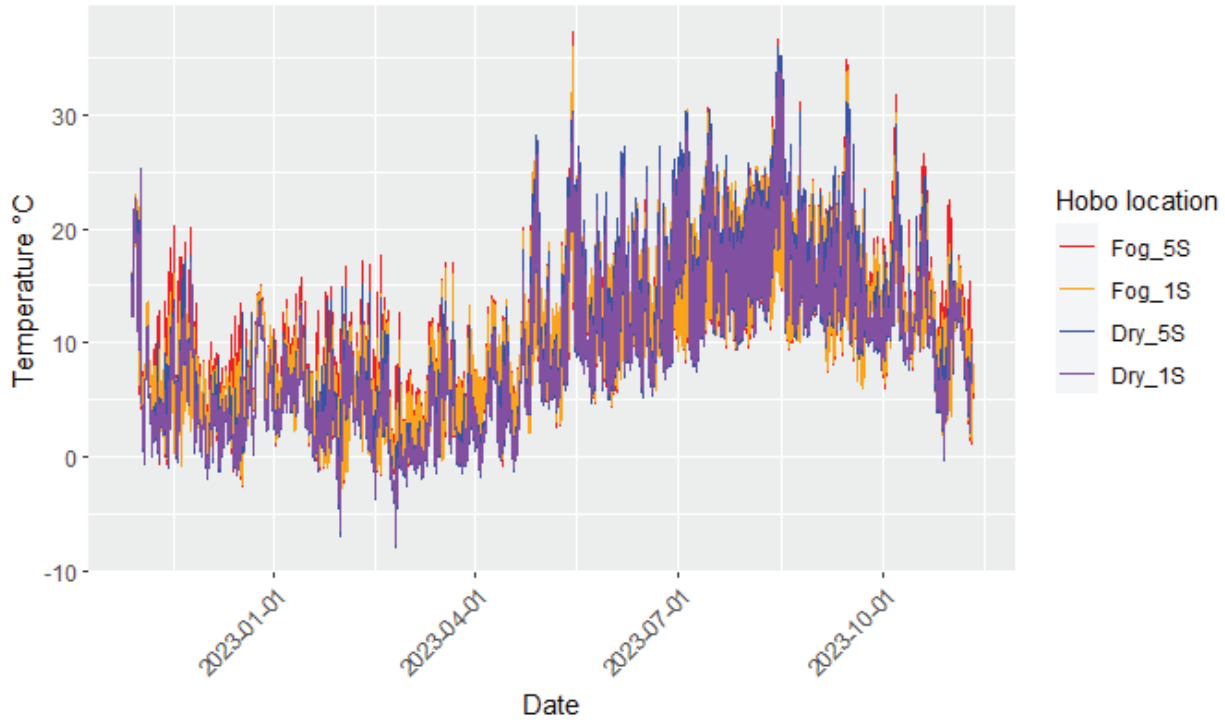
Temperature °C
30
20
10
0
-10
2023-01-01
2023-04-01
2023-07-01
2023-10-01
Date
Hobo location
Fog_5S
Fog_1S
Dry_5S
Dry_1S

(B)

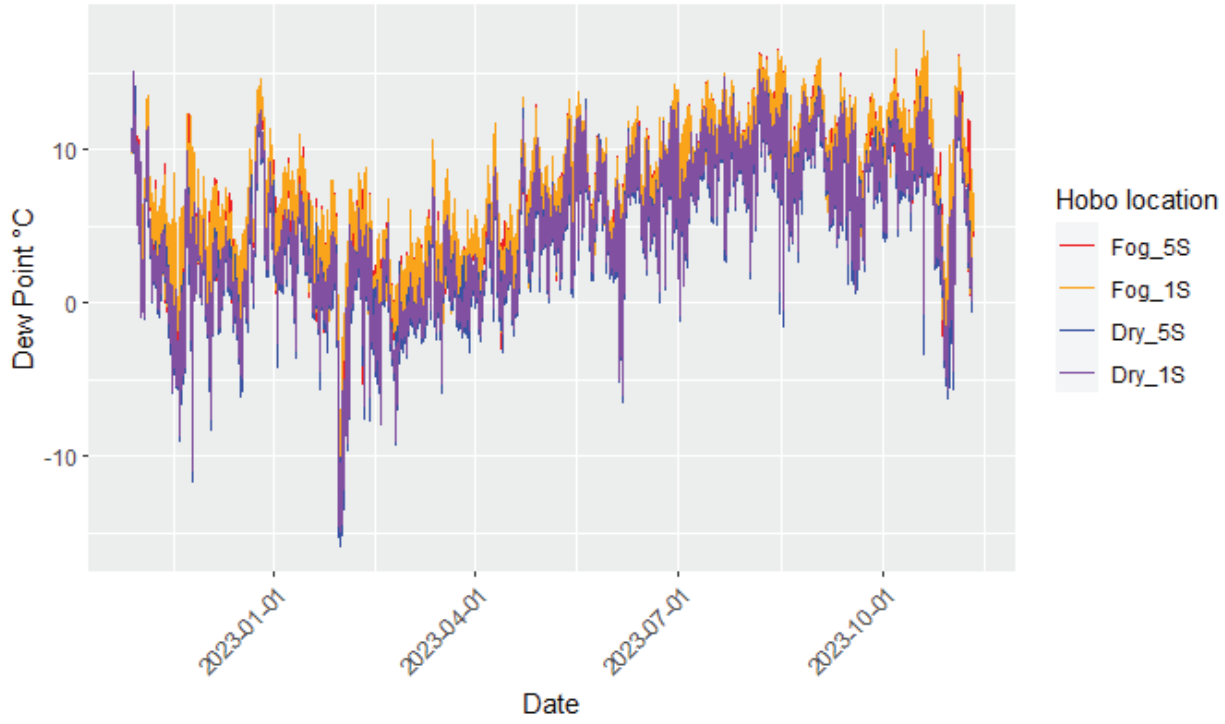
Dew Point °C
10
0
-10
2023-01-01
2023-04-01
2023-07-01
2023-10-01
Date
Hobo location
Fog_5S
Fog_1S
Dry_5S
Dry_1S

Figure 10. The temperature (A) and dewpoint temperature (B) of foggy and unfoggy sites, at the south facing of the lowest and the highest canopy positions. Numbers 1 and 5 represent the lowest and the highest canopy position, S represents the south-facing of the trees.

disease severity (% of stomata occluded) showed no clear trends based on crown third height. For the 13 CWHdm plots in the Fraser Valley, only lineage 1 was detected (no lineage 2).

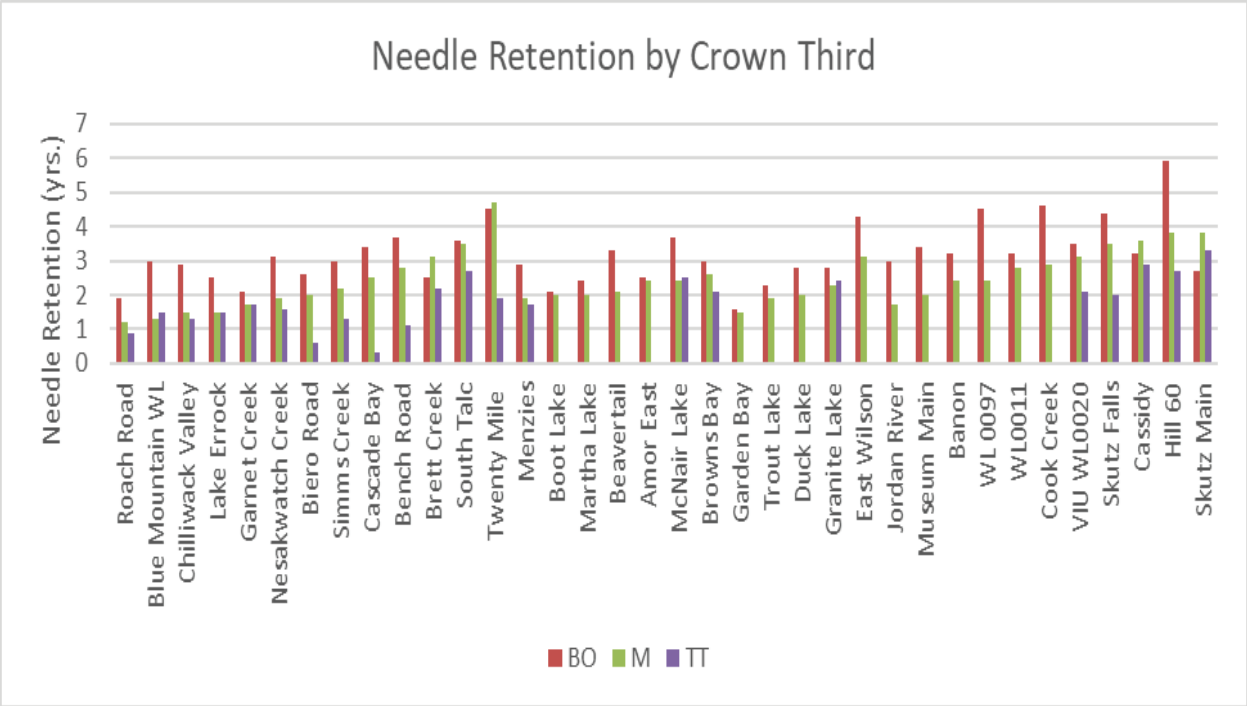

Figure 2. Needle Retention by Crown Third. BO = bottom, M=Middle, TT=top

No detailed analyses have been done yet, but scatter plots of various plot parameters (5-year growth, mid crown needle retention, 2nd year needle incidence, 2nd year needle severity, 2nd year colonization index, and elevation) were looked at for trends. Colonization index is defined as incidence x severity. The trends were quite different between the CWHdm and CWHxm plots. Five-year growth was negatively correlated with colonization index (as expected), but unrelated to mid crown needle retention in the CWHdm. In the CWHxm, there was an unexpected negative correlation between 5-year growth and needle retention and no correlation with colonization index, despite there being a negative correlation between 2nd year colonization index and mid crown needle retention as expected (r^2 =0.3). In the CWHdm there was a strong elevational trend with plots from higher elevation having better 5-year growth, better needle retention, and lower colonization index. No elevational trends were apparent for the CWHxm plots.

Acknowledgements: These plots were established by Stefan Zeglen (retired Ministry of Forests pathologist). Pseudothecial counts were done by UBC students under the direction of Dr. Richard Hamelin. Infinity-Pacific Stewardship Group Ltd. did the Chilliwack plot re-measurements and assisted with the foliar sampling for those plots.

In vitro suppression of the Swiss needle cast pathogen *Nothophaeocryptopus gaeumannii* by foliar endophytes of Douglas-fir

Hailey R. Graham[a], David R. McMullin[a], Joey B. Tanney[b*]

[a] Department of Chemistry, Carleton University, Ottawa, ON, K1S 5B6, Canada

[b] Pacific Forestry Centre, Canadian Forest Service, Natural Resources Canada, Victoria, BC, V8Z 1M5, Canada

Abstract

Douglas-fir (*Pseudotsuga menziesii*) is one of the most ecologically and economically important softwood trees grown worldwide. Over the last several decades in Oregon and Washington there has been a decline in Douglas-fir productivity due to infection of the endemic fungus *Nothophaeocryptopus gaeumannii* which causes the foliar disease Swiss needle cast. Conifer endophytes have previously been shown to produce toxins *in planta* capable of mitigating damage from herbivores and pathogens. An assay was developed to assess the antifungal properties of culture filtrate extracts from fifty-three Douglas-fir endophytes against *N. gaeumannii*. From these extracts, eight significantly inhibited the growth of at least one of three *N. gaeumannii* lineages studied. Further, the natural products from select strains were investigated. The aim of this study was to identify Douglas-fir endophyte extracts that inhibited the growth of *N. gaeumannii* to direct future investigations aimed at characterizing their antifungal natural products. Endophytes that inhibit *N. gaeumannii* are currently being prioritized for future studies to determine their potential in forest management applications.

Introduction

Swiss needle cast (SNC) is a foliar disease of Douglas-fir trees caused by the ascomycete fungus *Nothophaeocryptopus gaeumannii*, which is endemic to the Pacific Northwest (PNW, Ritóková et al. 2016; Lee et al. 2017). Prior to the mid-1970s, SNC did not have serious impacts on PNW forest productivity. It was not until the 1990s when aerial surveys illustrated that SNC infection had been intensifying, revealing approximately 200,000 hectares of symptomatic land in Oregon (Hansen et al. 2000; Ritóková et al. 2016). Since then, the disease continues to increase in severity, frequency, and range, expanding outside of plantations and into previously non-epidemic areas (Lee et al. 2017).

An unexplored potential strategy for controlling SNC severity in young plantations involves modulating the foliar microbiome to increase resistance to *N. gaeumannii* colonization and/or suppress pseudothecial development. Microbiomes contribute to plant health and development by, for example, enhancing nutrient acquisition, conferring biotic resistance via antagonism of pathogens and pests, and inducing tolerance to abiotic stresses (Singh et al. 2020; Lyu et al. 2021). A major component of plant microbiomes are fungal endophytes: ubiquitous and phylogenetically diverse fungi that are capable of asymptomatically colonizing plant tissue for all or part of their life history. Interactions between endophytes and their hosts can be complex and operate along the pathogen–mutualist continuum. Recently, there has been significant interest in harnessing endophytes for applications in agricultural systems as plant growth promoters and to reduce pests and pathogens (Poveda et al. 2021, Grabka et al. 2022). In terms of forestry applications, the best studied example is that of an endophyte strain of *Phialocephala scopiformis* (=*Mollisia scopiformis*), which produces the anti-insect toxin rugulosin. Spruce seedlings inoculated with this strain reduce the survival of the major defoliator eastern spruce budworm (*Choristoneura fumiferana*) and consequently decrease tree defoliation (Quiring et al. 2019a, b, Quiring et al. 2020). Seedlings inoculated in the greenhouse and out-planted in the field were still colonized by the endophyte more than eleven years after inoculation and were transmitted horizontally within canopies and to proximal natural regeneration (Miller et al. 2009, Frasz et al. 2014). Further, the *Pinus strobus* (white pine) endophytes *Xylaria ellisii* and a *Rhytismataceae* sp. produced antifungal compounds including griseofulvin and macrolides (Tanney et al. 2018). The macrolide

pyrenophorol inhibits the growth of the white pine pathogen *Cronartium ribicola*, the causal agent of white pine blister rust (Sumarah et al. 2015).

In this study we describe initial efforts to screen and identify foliar endophytes of Douglas-fir exhibiting *in vitro* antagonism to the causal agent of SNC, *N. gaeumannii*. The aim of this research is to discover target strains that may be inoculated into Douglas-fir seedlings and reduce the severity of SNC symptoms in the Pacific Northwest.

Materials and Methods

Collection of strains *Nothophaeocryptopus gaeumannii* strains were isolated according to the methods of Feau et al. (2024) (Figure 1). Douglas-fir endophytes were isolated from asymptomatic needles of various age classes collected from immature to old growth trees in managed to natural stands in coastal and interior British Columbia. Additional details describing the collection of *N. gaeumannii* and endophyte strains and their identification can be found in McMullin et al. 2017 and Tanney and Seifert 2018. Protocols describing the preparation of ethyl acetate soluble culture filtrate extracts and the characterization of purified natural products are reported by Graham 2023 (MSc thesis).

Inhibition of *N. gaeumannii* by endophyte extracts A 1 cm^2 portion of mature *N. gaeumannii* growing on 2% malt extract agar (MEA) supplemented with 0.2% yeast was aseptically macerated in sterile ddH_2O and used to inoculate (5% v/v) 250 mL Erlenmeyer flasks containing 50 mL of 2% malt extract broth supplemented with 0.2% yeast extract. Cultures were incubated stationary for 3 weeks at 20 °C. Douglas-fir endophyte culture filtrate extracts were dissolved in HPLC grade MeOH to a concentration of 50 mg mL^{-1} and applied to sterile 5 mm Whatman #1 disks in two 10 µL aliquots and left to dry for one hour. Excess media (8–16 mL) from the *N. gaeumannii* cultures was decanted from the flasks before macerating the cells. A 1 mm × 1 mm aliquot (25 µL) of the macerated cells was applied to the surface of 2% MEA supplemented with 0.2% yeast extract, allowing the excess media on the agar surface to dry (5–15 min). Once dry, disks containing the treatments were applied to the surface of the agar 1.5 cm away from the *N. gaeumannii* inoculum. Assays were performed in triplicate and incubated at 20 °C for 14 days. Nystatin (10 mg mL^{-1}) and HPLC grade MeOH were the positive and negative controls, respectively. After the 14-day incubation period, perpendicular diametral growth measurements (mm) were recorded and

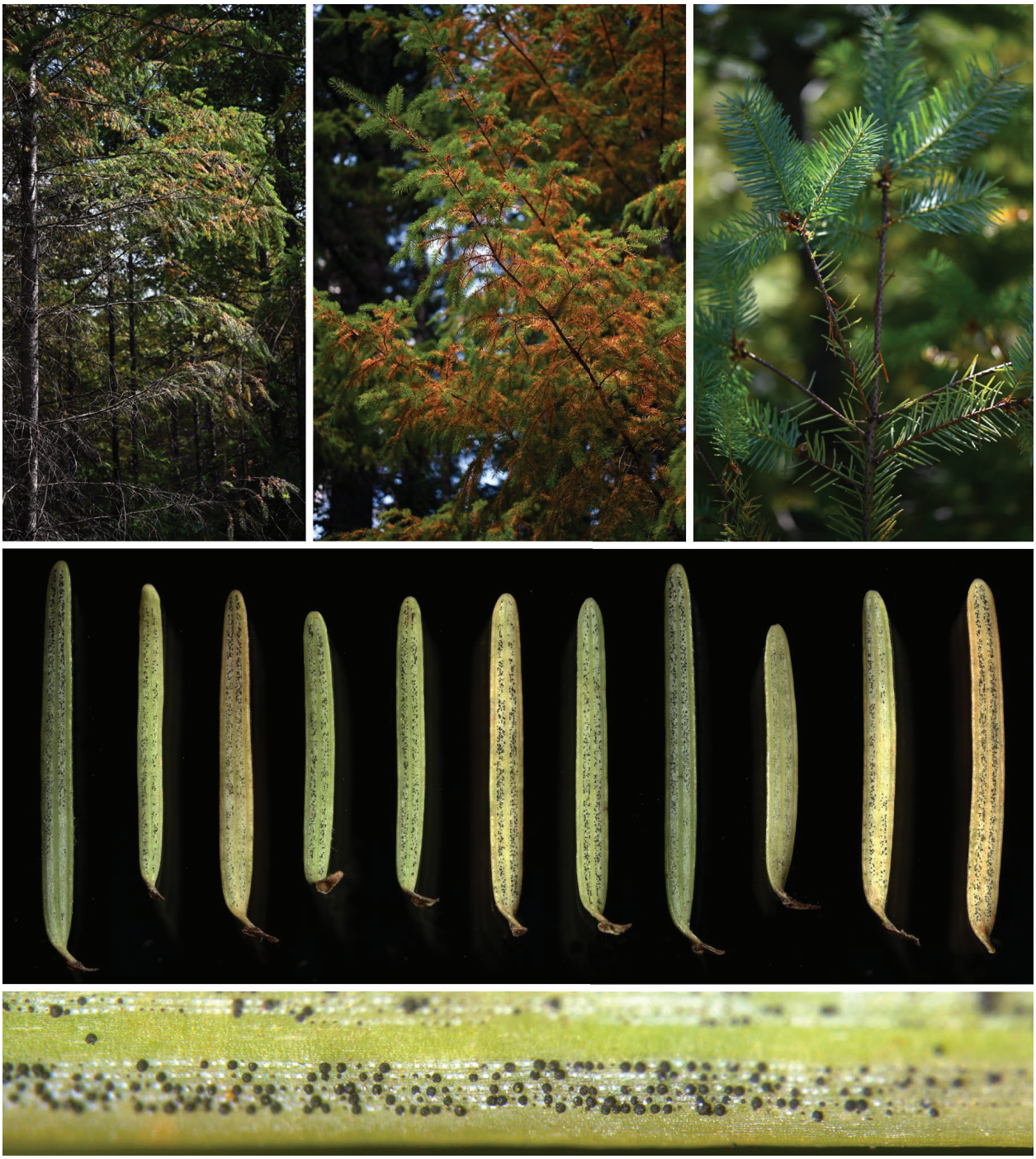

Figure 1. Top three photos of Douglas-fir trees showing classical symptoms of Swiss needle cast: low needle retention and chlorosis. Middle photo shows 11 needles showing varying chlorosis and stomata occluded by pseudothecia. Bottom photo shows close-up of stomata occluded by pseudothecia.

averaged. Each culture filtrate extract was tested against two representatives from each of the three *N. gaeumannii* lineages, lineage 1c, 1i and 2 (Feau et al. 2024). For each of the six *N. gaeumannii* strains tested, bioassay results were subjected to analysis of variance (ANOVA), and when significant ($p \leq 0.05$), treatment means were separated by Fisher's protected least significant difference test ($\alpha = 0.01$; Table 2). Statistical analysis was performed with JMP Pro 16.2 (SAS Institute, Cary, NC). Purified metabolites were also tested using the same procedure described above at 5 mg mL^{-1} against one representative from each of the three *N. gaeumannii* lineages.

Results and Discussion

The surface sterilization efficacy was confirmed by the absence of fungal growth on imprint plates and an overall high recovery rate of endophytes emerging from needle fragments. From one of the collection activities involving six sites, isolation plates for individual needles contained between (4–)5–12(–19) ($\bar{x} = 8$) needle fragments per plate and the average recovery rate of an endophyte per needle fragment ranged from 48.8–94.8% with an average recovery rate of 77.3–100% per whole needle (Table 1). For four of the six sites, all needles yielded at least one endophyte isolate. This collection across six sites included 13 trees and 280 needles, which yielded a total of 781 endophyte isolates emerging from needle fragments that, after sub-culturing of representative morphotypes, resulted in 293 strains selected for cultivation and preservation (Figure 2).

Table 1. Sampling statistics from a collecting activity involving six sites.

	Collection Site					
Statistic	**BLUE**	**CARO**	**COLQ**	**S3**	**THET**	**WITT**
Trees sampled	4	2	1	2	3	1
Needle samples	121	14	18	54	29	44
Endophyte isolates	256	53	72	215	91	94
Needles without growth	9	0	0	0	0	10
$\bar{x}$ recovery rate per needle fragment (%)	63.4	48.9	94.8	87.0	94.1	48.8
$\bar{x}$ recovery rate per needle (%)	92.6	100	100	100	100	77.3

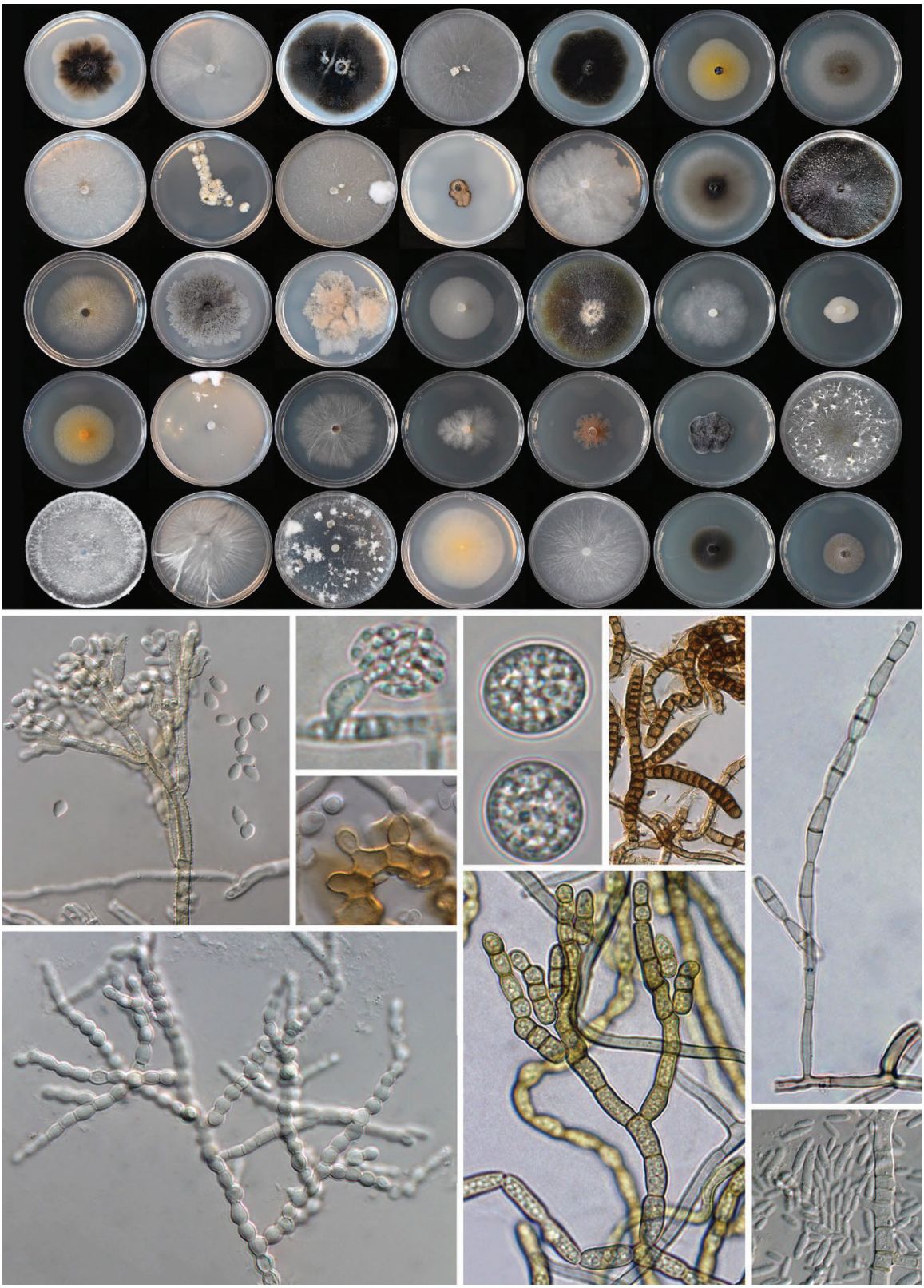

Figure 2. Examples of colony morphologies of Douglas-fir endophytes cultivated on 2% malt extract agar for three weeks (top photo) and morphologies of endophytes sporulating *in vitro*.

Representatives for each morphotype were identified by morphology and closest hits with identified ITS sequences in NCBI GenBank via BLASTn query. Fifty-three strains representing 32 unique taxa were selected based on criteria including taxonomic novelty, phylogenetic placement with other species known to produce antifungal natural products, and relative frequency. These strains were cultivated on liquid media for downstream work including antifungal assays and natural product characterizations. These 32 species represent 20 families in 14 orders across five classes.

Of the 53 Douglas-fir endophyte ethyl acetate soluble culture filtrate extracts tested, eight significantly inhibited the growth ($\alpha = 0.01$) of at least one of the six *N. gaeumannii* strains from the three lineages (Table 2). Notably, the extracts of *Lachnum virgineum* inhibited the growth of five of six *N. gaeumannii* strains tested and was statistically equal to the positive in all instances. The extracts from *Biscogniauxia* sp. nov. strains showed the most inhibition of *N. gaeumannii*. For example, these extracts inhibited 61 and 50% mycelial growth of *N. gaeumannii* lineage 1c strain 211, which were statistically the same as the positive control. Akin to one of the *Biscogniauxia* sp. nov. strains, the *Hypoxylon rubiginosum* extract also inhibited *N. gaeumannii* Lineage 1c and Lineage 1i. Ethyl acetate soluble culture filtrate extracts from *Pragmopora* cf. *piceae*, *Coniochaeta taeniospora*, *Xylariales* aff. *Linteromyces*, and *Mollisiaceae* sp. each inhibited the growth of a single *N. gaeumannii* strain. Some initial work into the metabolites of Douglas-fir endophytes is reported below. However, the strains identified in Table 2 inhibiting the growth of *N. gaeumannii* lineages will be comprehensively investigated to identify the major natural products responsible for the observed inhibition.

Table 2. Percent inhibition of *P. menziesii* endophyte crude extracts (50 mg mL^{-1}) on the mycelial growth of *N. gaeumannii* lineages. Values within a column connected by the same letter(s) are not statistically different according to Fisher's LSD test ($\alpha = 0.01$). Displayed values are significantly different from negative control.

	Lineage 1c		**Lineage 1i**		**Lineage 2**	
Endophyte extract	134	211	205	842	65	245
Negative control	bcdefghij	abcdefgh	abcdefghi	defghi	abc	ab
Positive control	69.1%, l	66.6%, l	62.6%, m	60.9%, j	51.3%, f	42.9%, e
Lachnum virgineum	40.5%, kl	47.1%, jkl	39.4%, lm		40.8%, ef	38.1%, e
Biscogniauxia sp. nov.		61.8%, l	39.4%, lm	28.6%, ij[a]		33.3%, de
Biscogniauxia sp. nov.		50.0%, kl	39.4%, lm			
Hypoxylon rubiginosum		41.2%, ijkl	39.4%, lm			
Pragmopora cf. *piceae*			30.3%, kl			
Xylariales aff. *Linteromyces*			27.3%, jkl			
Coniochaeta taeniospora					28.9%, def	
Mollisiaceae sp.						23.8%, cde

[a] Value statistically equal to positive and negative control.

While developing the assay to determine if culture filtrate extracts from Douglas-fir endophytes can inhibit the growth of *N. gaeumannii,* four strains were selected for initial investigations of their natural products (Figure 3). The strains were selected based on ethyl acetate soluble extract mass from initial cultivations, phylogenetic placement with species known to produce antifungal natural products, and relative frequency. From *Xylaria hypoxylon*, eight previously reported metabolites were characterized (Figure 3; **1-8**), many reliably known to be produced by the genus. Isolated natural products included the polyketides (*3R*)-5-hydroxymellein (**1**), its glucoside (**2**), xylarione A (**5**), griseofulvin (**7**) and dechlorogriseofulvin (**8**). Two small molecules (**9-10**) were produced by *Rhabdocline parkeri*. Several putative new tetronates were also purified and are currently undergoing full structural characterizations. Three small molecules including tyrosol (**4**) and scytalone (**12**) were purified from *Coleophoma* sp. nov. The low culture filtrate extract mass from *L. virgineum* (~17 mg L^{-1}) complicated purifying adequate amounts of compound for structural characterizations and antifungal activity assessment. Based on HRMS data, the *L. virgineum* strain that inhibited the growth of all three *N. gaeumannii* lineages identified in Table 2 produced several compounds (**13-20**), previously reported from the genus (Chang et al. 2016; Chu et al. 2023; Rukachaisirikul et al. 2006). Unfortunately, none of the purified metabolites inhibited the growth

of *N. gaeumannii,* even griseofulvin which is an active ingredient to treat fungal infections in humans. These *L. virgineum* metabolites represent molecules that should be assessed to determine which are responsible for inhibiting the growth of *N. gaeumannii*.

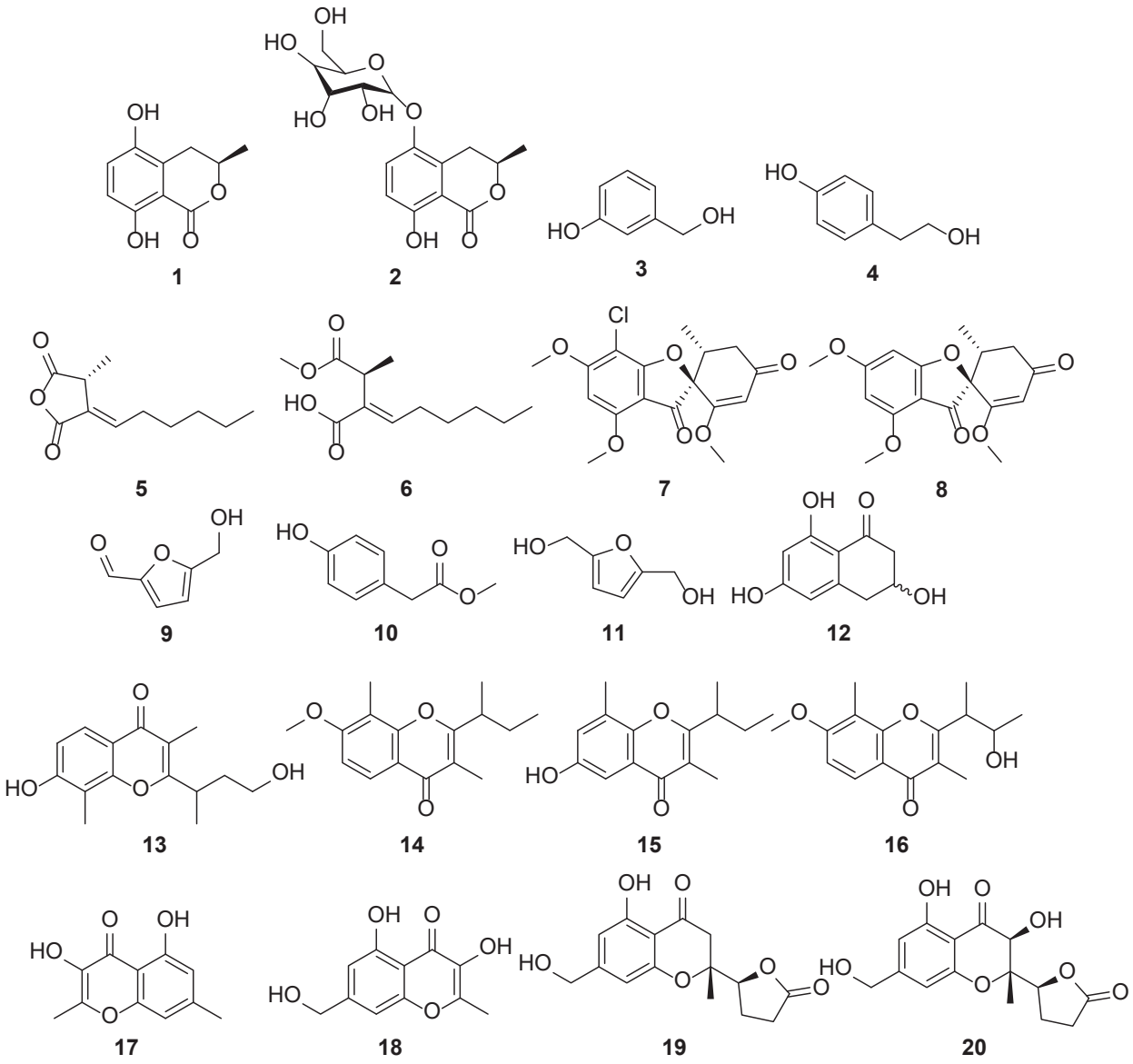

Figure 3. Chemical structures of natural products from studied endophyte culture filtrate extracts. Compounds (**1**–**8**) from *X. hypoxylon*, compounds (**9**–**10**) from *R. parkeri*, compounds (**4**,**11**–**12**) from *Coleophoma* sp. nov. and compounds (**13**–**20**) from *L. virgineum*.

This study provides initial results from a research project exploring the potential role of the Douglas-fir needle mycobiome in mediating the severity of SNC symptoms in younger plantations. Ongoing work involves: (1) using high-throughput metabarcoding to investigate differences in mycobiome profiles of asymptomatic versus symptomatic needles in sites where SNC is severe or negligible; (2) describing novel biodiversity; (3) characterizing bioactive natural products; and (4) expanding bioassays to include more taxa. We also anticipate a small pilot inoculation study to monitor SNC results in seedling inoculated with some of the endophyte strains described here. If successful, harnessing endemic fungi to reduce SNC symptoms may provide persistent protection long after inoculation and expand our available tools for climate change adaptation.

Acknowledgements

We thank Tyler Avis (Carleton University), Annie Dicaire (Canadian Forest Service) and Cameron D'Amours (University of Victoria) for technical assistance and helpful discussions with the project.

Contact us

Joey Tanney, PhD- joey.tanney@NRCan-RNCan.gc.ca
David McMullin, PhD- david.mcmullin@carleton.ca
Hailey Graham, MSc- HaileyGraham@cmail.carleton.ca

References

Chang, H. S., Lin, C. H., Chen, Y. S., Wang, H. C., Chan, H. Y., Hsieh, S. Y., Wu, H. C., Cheng, M. J., Yuan, G. F., Lin, S. Y., Lin, Y. J., & Chen, I. S. (2016). Secondary metabolites of the endophytic fungus *Lachnum abnorme* from *Ardisia cornudentata*. *International Journal of Molecular Sciences*, *17*(9). https://doi.org/10.3390/ijms17091512

Chu, J., Zhai, W., Geng, Y., Feng, Y., Wang, J., Li, J., Wang, Y., Zhuang, W., Che, Y., Li, Y., Chang, Z., & Ren, F. (2023). Lachnochromonin, a fungal metabolite from *Lachnum virgineum*, inhibits cell growth and promotes apoptosis in tumor cells through JAK/STAT3 signaling. *Cellular Signalling*, *106*. https://doi.org/10.1016/j.cellsig.2023.110592

Feau, N., Tanney, J. B., Herath, P., Leal, I., & Hamelin, R. C. (2024). Genome sequences of three genetic lineages of the fungus *Nothophaeocryptopus gaeumannii,* the causal agent of Swiss needle cast on Douglas-fir trees. *Microbiology Resource Announcements*, *13*(2). https://doi.org/10.1128/mra.01008-23

Frasz, S. L., Walker, A. K., Nsiama, T. K., Adams, G. W., & Miller, J. D. (2014). Distribution of the foliar fungal endophyte *Phialocephala scopiformis* and its toxin in the crown of a mature white spruce tree as revealed by chemical and qPCR analyses. *Canadian Journal of Forest Research*, *44*(9), 1138–1143. https://doi.org/10.1139/cjfr-2014-0171

Grabka, R., d'Entremont, T. W., Adams, S. J., Walker, A. K., Tanney, J. B., Abbasi, P. A., & Ali, S. (2022). Fungal endophytes and their role in agricultural plant protection against pests and pathogens. *Plants*, *11*(3), 384. https://doi.org/10.3390/plants11030384

Hansen, E. M., Stone, J. K., Capitano, B. R., Rosso, P., Sutton, W., Winton, L., Kanaskie, A., & McWilliams, M. G. (2000). Incidence and impact of Swiss needle cast in forest plantations of Douglas-fir in coastal Oregon. *Plant Disease*, *84*(7), 773–778. https://doi.org/10.1094/PDIS.2000.84.7.773

Lee, E. H., Beedlow, P. A., Waschmann, R. S., Tingey, D. T., Cline, S., Bollman, M., Wickham, C., & Carlile, C. (2017). Regional patterns of increasing Swiss needle cast impacts on Douglas-fir growth with warming temperatures. *Ecology and Evolution*, *7*(24), 11167–11196. https://doi.org/10.1002/ece3.3573

Lyu, D., Zajonc, J., Pagé, A., Tanney, C. A. S., Shah, A., Monjezi, N., Msimbira, L. A., Antar, M., Nazari, M., Backer, R., & Smith, D. L. (2021). Plant holobiont theory: the phytomicrobiome plays a central role in evolution and success. *Microorganisms*, *9*(4), 675. https://doi.org/10.3390/microorganisms9040675

McMullin, D. R., Green, B. D., Prince, N. C., Tanney, J. B., & Miller, J. D. (2017). Natural products of *Picea* endophytes from the Acadian Forest. *Journal of Natural Products*, *80*(5), 1475–1483. https://doi.org/10.1021/acs.jnatprod.6b01157

Miller, J. D., Cherid, H., Sumarah, M. W., & Adams, G. W. (2009). Horizontal transmission of the *Picea glauca* foliar endophyte *Phialocephala scopiformis* CBS 120377. *Fungal Ecology*, *2*(2), 98–101. https://doi.org/10.1016/j.funeco.2009.01.002

Poveda, J., Eugui, D., Abril-Urías, P., & Velasco, P. (2021). Endophytic fungi as direct plant growth promoters for sustainable agricultural production. *Symbiosis*, *85*(1), 1–19. https://doi.org/10.1007/s13199-021-00789-x

Quiring, D., Adams, G., Flaherty, L., McCartney, A., Miller, J. D., & Edwards, S. (2019a). Influence of a foliar endophyte and budburst phenology on survival of wild and laboratory-reared eastern spruce budworm, *Choristoneura fumiferana* on white spruce (*Picea glauca*). *Forests*, *10*(6), 503. https://doi.org/10.3390/f10060503

Quiring, D., Adams, G., McCartney, A., Edwards, S., & Miller, J. D. (2020). A foliar endophyte of white spruce reduces survival of the eastern spruce budworm and tree defoliation. *Forests*, *11*(6), 659. https://doi.org/10.3390/f11060659

Quiring, D., Flaherty, L., Adams, G., McCartney, A., Miller, J. D., & Edwards, S. (2019b). An endophytic fungus interacts with crown level and larval density to reduce the survival of eastern spruce budworm, *Choristoneura fumiferana* (*Lepidoptera: Tortricidae*), on white spruce (*Picea glauca*). *Canadian Journal of Forest Research*, *49*(3), 221–227. https://doi.org/10.1139/cjfr-2018-0194

Ritóková, G., Shaw, D., Filip, G., Kanaskie, A., Browning, J., & Norlander, D. (2016). Swiss needle cast in western Oregon douglas-fir plantations: 20-Year Monitoring Results. *Forests*, *7*(12), 155. https://doi.org/10.3390/f7080155

Rukachaisirikul, V., Chantaruk, S., Pongcharoen, W., Isaka, M., & Lapanun, S. (2006). Chromone derivatives from the filamentous fungus *Lachnum* sp. BCC 2424. *Journal of Natural Products*, *69*(6), 980–982. https://doi.org/10.1021/np060164e

Singh, S., Kumar, V., Dhanjal, D. S., Sidhu, G. K., Datta, S., Kumar, S., & Singh, J. (2020). Endophytic microbes in abiotic stress management. In A. Kumar & V. K. Singh (Eds.), *Microbial Endophytes* (pp. 91–123). Elsevier. https://doi.org/10.1016/B978-0-12-818734-0.00005-X

Sumarah, M. W., Walker, A. K., Seifert, K. A., Todorov, A., & Miller, J. D. (2015). Screening of fungal endophytes isolated from eastern white pine needles. In R. Jetter (Ed.), *The Formation, Structure and Activity of Phytochemicals* (pp. 195–206). Springer International Publishing. https://doi.org/10.1007/978-3-319-20397-3_8

Tanney, J. B., McMullin, D. R., & Miller, J. D. (2018). Toxigenic foliar endophytes from the Acadian Forest. In A. Pirttilä & A. Frank (Eds.), *Endophytes of forest trees: biology and applications* (Vol. 86, pp. 343–381). https://doi.org/10.1007/978-3-319-89833-9_15

Tanney, J. B., & Seifert, K. A. (2018). *Phacidiaceae* endophytes of *Picea rubens* in eastern Canada. *Botany*, *96*(9), 555–588. https://doi.org/10.1139/cjb-2018-0061

Forest Ecology and Management 537 (2023) 120930

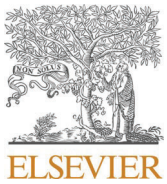

Contents lists available at ScienceDirect

Forest Ecology and Management

journal homepage: www.elsevier.com/locate/foreco

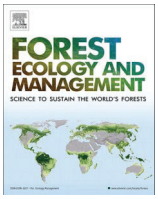

Site-level estimates of Douglas-fir foliage retention from climate, soil, and topographic variables

Douglas B. Mainwaring [a,*], Gabriela Ritóková [b], David C. Shaw [c], Rachel K. Brooks [d], Daniel W. Omdal [d]

[a] Department of Forest Engineering, Resources, and Management, Oregon State University, 319 Peavy Forest Science Center, Corvallis, OR 97331, United States
[b] Oregon Department of Forestry, United States
[c] Department of Forest Engineering, Resources, and Management, Oregon State University, United States
[d] Washington Department of Natural Resources, United States

ARTICLE INFO

Keywords:
Swiss needle cast
Douglas-fir
Forest health

ABSTRACT

Cohort-based live foliage retention of Douglas-fir (*Pseudotsuga menziesii*), repeatedly shown to be directly related to tree growth, was estimated for areas in western Oregon and Washington by correlating nearly 1000 plot-level estimates of foliage retention with variables of climate, soils, and topography. Sampling of Douglas-fir foliage retention, motivated by the Swiss needle cast-induced loss of foliage (causal agent *Nothophaeocryptopus gaeumanii*) in western Oregon and Washington, covered the period from 1998 to 2021, with estimates collected from the Oregon Coast Range near the California border to the Olympic Peninsula and the foothills of the northern Oregon Cascades and the foothills near the border of Washington and Canada. Douglas-fir foliage retention was found to be correlated with average June/July relative humidity, December maximum temperature, and May precipitation averaged for the periods of budbreak for the 2–4 yr old needle cohorts, a transformation of slope and aspect, the number of meters above 400 m elevation, topographic position index, and soil cation exchange capacity. Using the constructed equation, foliage retention was estimated across a systematic grid of points in western Oregon and Washington and combined with a regional growth model to estimate potential volume growth loss across the region. The greatest implied average growth losses (~23%) were in the zones closest to the Pacific Ocean between 46° and 48°N. Premature loss of Douglas-fir foliage in the Pacific Northwest has been primarily associated with Swiss needle cast, and this work may help explain conditions that favor Swiss needle cast or describe additional foliage retention drivers.

1. Introduction

Douglas-fir (*Pseudotsuga menziesii*) foliage retention, typically measured by the number of years of retained foliage cohorts, has repeatedly been shown to have a high correlation with diameter or height increment or volume production (Maguire et al. 2002, Maguire et al. 2011). While this variable has been shown to be influenced by factors such as site fertility (Gower et al. 1992, Balster and Marshall 2000) and elevation (Shaw et al. 2014, Ritóková et al. 2016), more recent examination of its role in Douglas-fir productivity has shown that it has mainly been due to the influence of Swiss needle cast (SNC) disease in western Oregon, USA (Ritóková et al. 2016, Ritóková et al. 2021, Shaw et al. 2021).

Swiss needle cast is an endemic foliar disease specific to Douglas-fir, and has been at epidemic levels along large portions of the northern Pacific coast of North America since the 1990s (Hansen et al. 2000, Shaw et al. 2021). Caused by the ascomycete *Nothophaeocryptopus gaeumanii*, successful infection of newly developing Douglas-fir foliage takes place in the spring and early- mid summer, during and shortly after shoot elongation (Hansen et al. 2000). Fungal development results in the production of fruiting bodies called pseudothecia, which block gas exchange by plugging needle stomates, resulting in needle death and abscission (Manter et al. 2000) and reduced diameter and height increment (Maguire et al. 2002).

The Douglas-fir resource is quite valuable, and is central to the forest products economy of the region, therefore, the observed effect of foliage loss on the condition of trees and stands in the coastal region resulted in a cooperative research effort to understand SNC's disease biology,

* Corresponding author.
E-mail address: Doug.mainwaring@oregonstate.edu (D.B. Mainwaring).

https://doi.org/10.1016/j.foreco.2023.120930
Received 23 January 2023; Received in revised form 8 March 2023; Accepted 10 March 2023
Available online 28 March 2023

epidemiology, effects on wood properties and growth and yield, as well as tree and stand response to typical or possibly disease-alleviating silvicultural treatments (Shaw et al. 2011; see https://sncc.forestry.oregonstate.edu/publications). While this effort has produced a solid understanding of the disease and its interaction with its Douglas-fir host, the non-cyclic consistency of disease symptoms throughout the epidemic area in the last 25 years has shown that silvicultural tools provide an ineffective means for managing SNC, and that management needs to adjust to the disease.

Because "needle cast" or foliage loss is the primary symptom of the disease, any estimation of SNC-related growth loss on the tree, stand, or landscape scale using existing equations or tools requires an estimation of foliage retention. While the recommended method of obtaining an estimate of foliage retention involves estimating values on individual trees, this is not realistic for larger scales, such as populating entire inventories, for bare ground where no symptomatic trees exist, or for acquisitions where this data isn't available. In examples such as these, equations that can predict potential foliage retention from site specific data are critical for informing landowners or managers about potential productivity or financial return.

Epidemiological research has identified climate factors that are especially influential in the successful germination and development of *N. gaeumannii* (Rosso and Hansen 2003, Manter et al. 2003, Manter et al. 2005). Elevation-interpolated climate variables, easily downloadable by inputting latitude and longitude using web-based tools (Wang et al. 2016), have made it possible to correlate measured foliage retention with year-specific estimates of different climate variables of different temporal scales. Multiple climate-based Douglas-fir foliage retention models (Coop and Stone 2007, Latta et al. 2010, Zhao et al. 2011) were created more than 10 years ago based on foliage retentions estimated during the 1998–2009 period throughout the northern Oregon Coast Range, the region with the greatest concentration of SNC symptoms at that time. Each model utilized a different set of predictor variables or statistical techniques and a slightly different dataset to produce a foliage retention model that could be applied across western Oregon and Washington from downloadable variables.

Site specific foliage retention estimates of each model were slightly different, with the greatest differences being in comparisons between the northern versus southern Oregon coast. Importantly, ~88% of the measured foliage retentions used for construction of these models were collected from stands north of Newport, Oregon and south of Astoria, Oregon, accounting for only ~ 27% of the north–south distance from the Oregon-California border to Neah Bay, the northern-most point of Washington's Olympic Peninsula. Since the collection of the original dataset, the geographic extension of SNC symptoms has resulted in an expansion of the foliage retention sampling area, including the establishment of a new SNC research plot network throughout the entire Oregon Coast Range (Shaw et al. 2021), establishment of a periodic SNC aerial survey and associated ground truth sampling to Washington state, and a set of transects established within young plantations in the foothills of the Oregon Cascades, and monitoring in British Columbia, Canada. This additional sampling has increased both the spatial and temporal scale of the foliage retention database, heightening the value of refitting a regional model of foliage retention.

The value of site-specific estimates of foliage retention is enhanced by improvements in the availability and ease of extraction of numerous potential predictor variables from custom rasters. Rapid extraction of data for specific latitudes and longitudes corresponding to specific stands, calculation of foliage retention, and application within a growth and yield model in combination with existing SNC increment modifiers will result in a powerful decision support tool for estimating volume yield and the financial reality of managing Douglas-fir in the presence of SNC. This paper describes the development of a site-specific model of foliage retention with a well distributed dataset covering the range of SNC-symptoms, and its application within the most affected zones of the same region to estimate volume growth losses.

2. Methods

2.1. Data

2.1.1. Sites

A large multi-year dataset was assembled from multiple separate studies and efforts (Fig. 1, Table 1.):

SNCC Growth Impact study (GIS): Located across the NW Oregon Coast Range, foliage retention assessments were made annually from 1998 to 2003, and again in 2005 and 2008 as part of the original SNCC monitoring network (Maguire et al. 2011).

SNCC Pre-commercial thinning study (PCT): Located across the NW Oregon Coast Range, foliage retention assessments were made annually from 1998 to 2003, and again in 2005 and 2008 as part of the original pre-commercial thinning study (Mainwaring and Maguire 2008).

SNC Commercial thinning study (RCT and CT): Located across the NW Oregon Coast Range and Cascades foothills, a retrospective component (RCT) of this study was assessed twice in 2002 and 2006 or 2003 and 2007, and permanent pairs (CT) were assessed three times in 2002, 2004, and 2006 or 2003, 2005, and 2007 (Mainwaring et al. 2007).

USFS Cascades transects (CASCT1): Located across the northern Oregon Cascades, these plots were assessed annually in 2001, 2002, and 2003 (Freeman 2002).

SNCC Research plot network study (RPN): Located across the Oregon Coast Range and SW Washington Coast Range, these plots were each assessed twice in the mid and late 2010 s (Ritóková et al. 2021).

SNCC Cascades transects (CASCT2): Located across the northern Oregon Cascades foothills, these transects were assessed approximately annually from 2017 to 2020 (Ritóková and Shaw 2020).

WDNR SNC monitoring (WDNR): Located across the Washington Coast Range, these transects were assessed periodically between 2011 and 2021 (Brooks and Omdal 2021, Herpin-Saunier et al. 2022).

SNCC Coastal transects (SOT and WT): Located across the central Oregon Coast Range and also the SW Washington Coast Range, these

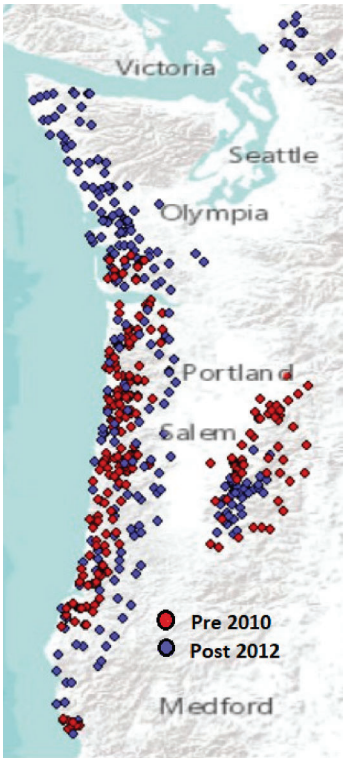

Fig. 1. Location of SNC sample points, 1998–2021.

Table 1
Summary data for projects and variables in included in the final modeling dataset.

Project	N	Type	Year	RH07 (%)	TMAX, Dec. (°C)	PPT, May (mm)	Slope (%)	Aspect (°)	MA400 (m)	TPI	CEC ($cmol_c$/kg)
BN	4	mean	2008	60	8	86.8	19.6	131	0	0.1	33.1
	4	max	2010	67.7	9.7	128.7	40.3	194	0	12	57
	4	min	2007	51	6.6	45	11.2	39	0	−11.3	12.4
CASCT1	46	mean	2002	58.8	6.7	161.6	19.8	207	248	3.2	25
	46	max	2003	66.3	8.5	221.7	54.1	360	835	28.7	47
	46	min	2001	47.3	4.3	104	0.4	3	0	–23.6	12.8
CASCT2	46	mean	2018	55	6.8	84.1	20.1	201	71	4.4	18.5
	46	max	2020	60	8.3	132.7	54.1	359	385	39.3	30.7
	46	min	2017	48.3	5.4	50.3	1.9	3	0	−12.1	13.3
CT	30	mean	2005	59.8	8.7	114.1	47.1	202	4	8.5	27.6
	30	max	2007	65.3	10	159.3	63.4	345	63	26.6	40.6
	30	min	2002	53.3	5.2	62	16	47	0	−17.7	15.7
WDNR	165	mean	2016	66	7	103.9	11.6	191	4	1.9	38.6
	165	max	2021	77.7	9.4	234.3	66.5	359	165	23.7	55
	165	min	2011	54.7	4.4	43	0.1	7	0	−12.5	2.9
GIS	232	mean	2003	65	8.4	134.8	30	184	15	2.4	43.6
	232	max	2008	74.7	10.5	248.3	85.8	349	529	39.8	55.6
	232	min	1998	52.7	5.5	65.7	1.8	11	0	–32.7	10.9
Menasha	1	mean	2004	65	12.4	60.7	23.6	135	0	−1.3	53.2
	1	max	2004	65	12.4	60.7	23.6	135	0	−1.3	53.2
	1	min	2004	65	12.4	60.7	23.6	135	0	−1.3	53.2
PCT	142	mean	2003	62.3	8.1	121.4	29.6	211	16	7.8	38.8
	142	max	2008	73.7	9.9	195.3	67	358	355	25.7	55.5
	142	min	1998	52.7	5.1	68.3	3.6	0	0	−11.8	14.4
RCT	20	mean	2004	63.7	8.9	119.6	30.4	182	56	2.3	30.6
	20	max	2007	74.3	10.1	194	71.2	357	332	14.6	37
	20	min	2002	54	6.6	59	10.7	47	0	–32.2	15.7
RPN	206	mean	2018	62.1	8	94.8	24.2	153	40	6.6	31.9
	206	max	2021	76.3	11.8	224.3	63.1	359	407	34.2	60
	206	min	2014	51	4	28	3.2	1	0	−21.6	5.1
SOT	52	mean	2009	63.2	9.7	117	23.6	185	19	11.7	25.9
	52	max	2009	71.7	11.8	158.7	89	358	222	38.1	60
	52	min	2009	51.7	8.1	89.7	1.4	1	0	–22.6	11.2
WT	10	mean	2009	66.3	7.9	115.5	13.9	159	0	8.7	40.2
	10	max	2009	72	8.6	136	28.9	333	0	32.2	55
	10	min	2009	63	7.5	93.3	1.9	16	0	−4.5	12.2

transects were assessed in 2009 (Shaw and Woolley 2009).

Beyond N fertilizer trials (BN): Located at four sites sampled as part of the Beyond N fertilization trials, and assessed in 2007 and 2008 (Mainwaring et al. 2014).

Menasha silvicultural trials (Menasha): Located at a single site near Coos Bay, Oregon and assessed in 2004 (Mainwaring et al. 2004).

2.2. Foliage retention

Foliage retention measurement protocols call for the estimation of foliage retention on 5–10 dominant trees per plot, with assessments based on secondary lateral branches of the mid-crown. Assessments have been made from the ground, with or without binoculars based on tree size, and from visual inspection of branches collected by climbing trees.

Tree-level foliage retention was estimated two different ways, either as the sum of the proportion retained foliage on individual cohorts of sampled branches, or when crown observation is more difficult, a tree-level average from multiple observed branches. Because the more recent foliage retention sampling efforts were based on a four-year-old secondary branch (thus limiting the maximum foliage retention to 4.0 years), the analysis dataset was limited to those earlier sites with foliage retentions reported by annual cohort, or those with a total foliage retention of no more than 3.5 years, under the assumption that total average foliage retentions of that amount could be confidently assumed to be limited to the first four annual cohorts.

Numerous older stands sampled as part of the SNC Commercial thinning project were within the zone of the Tillamook burns of the 1930 s −1950 s. The massive reforestation effort following these burns were believed to include seed sources from areas now understood to be inappropriate for that area (Hansen et al. 2000). Accordingly, data from older stands of this region were not used, based on the desire to be able to estimate foliage retention for region-appropriate stock.

2.3. Climate and topography

Annual, seasonal, and monthly climate variables for each year between 1994 and 2021 were generated for each site within the dataset using ClimateNA (v7.20, Wang et al. 2016). A 30 m DEM was created for western Oregon and Washington using Google Earth Engine. This DEM was used in R v4.1.0 (R Core Team 2021) within the RSAGA package (Brenning et al. 2018) to create rasters for slope, aspect, topographic position index (TPI) and topographic wetness index (TWI). Both indices account for neighboring topography to describe local concavity (negative value) or convexity (positive value). These DEM-estimated variables were used for each site if it were otherwise unrecorded.

2.4. Soils

A Natural Resource Conservation Service (NRCS) soil mapunit raster was made within ARCMAP 10.8.1 (ESRI, Redlands, CA, U.S.). This was coupled with a dataset containing specific NRCS soil variables (organic matter, cation exchange capacity, available water content, pH, sand %, silt %, clay %, and numerous soil particle size class contents) for each mapunit.

2.5. Analysis

Identification of significant climate predictor variables from among ClimateNA output (min, max, and average temperature, maximum temperature difference, relative humidity, vapor pressure deficit, precipitation, Hargreaves climatic-moisture deficit, Hargreaves reference

evaporation, Hoggs climate moisture index) was first conducted using foliage retention data from 2 to 4 year old annual cohorts and an all-subsets linear regression within SAS v9.4 (SAS institute, Cary N.C, USA) which accounted for years since bud break (2, 3, or 4 yrs). First year foliage retention was excluded from this exploratory analysis because even in the most infected stands, 1-year old foliage is mostly entirely retained.

Although annual, seasonal and monthly climate variables were available for analysis, the analysis focused on monthly climate variables because of its previously identified superiority of prediction (Zhao et al. 2011). The variables identified during the abovementioned all-subsets regression as most correlated with foliage retention generally conformed to previously published information about the epidemiology of SNC: spring and early summer moisture during the time of Douglas-fir budbreak (important for successful fungal germination) and winter temperature (important for overwinter fungal development) (Manter et al. 2003). Accordingly, the monthly data was lagged so that spring moisture-related variables for predicting the foliage retention of a given cohort were specific to the year of that cohort's emergence. Likewise, temperature-related variables were lagged to be timed with the period immediately following budbreak (November or December temperatures of the year of budbreak, Jan-March temperatures of the following year).

Following identification of the most highly correlated climate variables using all subsets linear regression (average June and July relative humidity, December maximum temperature, May precipitation), additional topographic and soil variables were added to identify those with the greatest correlation.

Once the most correlated variables were chosen, a non-linear model of the following form was constructed for prediction of average plot-level foliage retention:

$$FR = 4 \bullet (1 - exp(a_0 + a_1 \bullet X_1 + a_2 \bullet X_2 + \cdots a_n \bullet X_n)) \quad (1)$$

where FR was average plot foliage retention, $X_{1\ldots n}$ were predictor variables and a_0-a_n were parameters estimated from the data. Because the youngest cohort of foliage generally exhibits full retention regardless of SNC level, the chosen climate variables were the average of the lagged values for 2–4 year old cohorts. For example, the average June-July relative humidity (RH_{67}) used within equation [1] for foliage assessed in 2010 would be (RH_{67}_2008 + RH_{67}_2007 + RH_{67}_2006)/3.

It was necessary to account for topographic variables because ClimateNA produces elevation-interpolated estimates, but doesn't otherwise account for topography. Topographic variables included a slope-aspect transformation (Stage 1976), and the RSAGA-estimated TPI and TWI, inclusion of which was based on early Swiss needle cast research (Rosso and Hansen 2003). A newer and more sophisticated slope-aspect transformation (Stage and Salas 2007) was not considered because the elevation component was already accounted for with the climate data.

Because of repeated measurement of many of the plots (up to 8 observations in 11 years), the multiple observations could not be considered independent. An earlier analysis (Zhao et al. 2011) addressed autocorrelation by using a random plot variable within the mixed effects analysis. Out of concern that this technique would impact the quantitative influence of plot-specific climate and topographical factors, independence among observations was addressed through subsetting the modeling dataset. The limited lifespan of specific needle cohorts equates to full periodic replacement of foliage on all trees. If measurements are spaced adequately in time, the same trees have an entirely different set of needles, without temporal overlap. Accordingly, the dataset was subsetted, limiting multiple observations of a given plot to a minimum interval of four years, unless SNC levels were sufficiently high. For the 128 plots of the GIS and PCT datasets, for which eight observations per plot were available (1998–2003, 2005, 2008), for most plots only the 1998, 2003, and 2008 observations were retained. If the foliage retention within these plots was consistently below 2.0 years, a three-year measurement interval was considered adequate for relative independence among measurements. For these plots, the 1998, 2001, 2005 and 2008 observations were retained. For datasets with multiple measurements within a four-year period, specific measurements were randomly chosen for inclusion within the modeling dataset. Unused observations for modeling (46.4% of the total) were used to validate the results of the final model.

The final model for predicting average plot foliage retention, using 53.6% of the total observations, was:

$$FR = 4 \bullet (1 - \exp(a_0 + a_1 \bullet RH_{67} + a_2 \bullet TMAX_{12} + a_3 \bullet PPT_{05} + a_4 \bullet slope \bullet \cos(asp) + a_5 \bullet slope \bullet \sin(asp) + a_6 \bullet MA400^{0.5} + a_7 \bullet TPI + a_8 \bullet CEC^{0.5})) \quad (2)$$

where RH_{67} is average June and July relative humidity (%), $TMAX_{12}$ is December max temperature (°C), PPT_{05} is average May precipitation (mm), slope is in radians, aspect is in radians, MA400 is meters above 400 (0 if elevation ≤ 400 m and (elevation – 400) if elevation > 400 m), TPI is topographic position index, based on a radius of 200 m, and CEC is soil cation exchange capacity (meq/100 g).

Geographic distribution of predicted results was produced by extracting significant predictor variables from constructed rasters across a 400 m systematic grid of points in western Oregon and Washington. Climate predictions were based on decadal averages (2010–2020).

2.6. Yield estimates

Yield estimates for uninfected Douglas-fir at age 50 years were obtained using a regional proprietary growth model created by the Center for Intensive Planted-forest Silviculture at Oregon State University (CIPSANON). Yields were produced by projecting a 5-year old treelist from a Douglas-fir plantation that had been subjected to two years of weed control. For the simulation, projections used a 50-yr site index of 120 ft (Bruce 1981), and foliage retentions of 1.5–3.0 years in 0.1 year increments. The effect of foliar loss on individual tree growth within CIPSANON is based on separate height and diameter multipliers with an increment adjustment that is a function of foliage retention (Mainwaring et al. 2020). A separate adjustment is made on final volume estimates by accounting for differences in stem form, also based on a function of foliage retention (Mainwaring and Maguire 2020). Final yields from each projection were based on 12.2 m log lengths, a 4.9 m minimum log length, and a minimum top diameter of 10 cm.

3. Results

Parameter estimates and standard errors for equation [2] are shown in Table 2 and residuals versus predicted values is shown in Fig. 2. Figs. 3-5, based on the same y-axis scale, provide a graphical picture of the relative response of foliage retention to each of the predictor variables over the range of the predictor variables within the dataset.

Douglas-fir foliage retention was estimated to decrease with increasing June and July relative humidity, varying up to one year across the range of dataset RH (Fig. 3a). Likewise, foliage retention

Table 2
Parameter estimates and standard errors from fit to equation [2].

Parameter	Estimate	SE
a_0	−3.2698	0.1473
a_1	0.0269	0.00249
a_2	0.0266	0.00781
a_3	0.00144	0.000292
a_4	−0.136	0.0431
a_5	−0.1261	0.0581
a_6	−0.0337	0.00335
a_7	0.00273	0.000835
a_8	0.033	0.00883

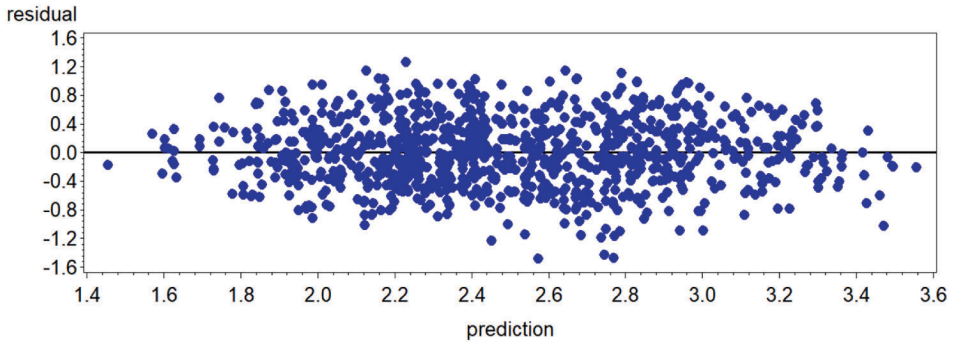

Fig. 2. Residuals versus predicted values from fitting equation [2] to the final (subsetted) dataset.

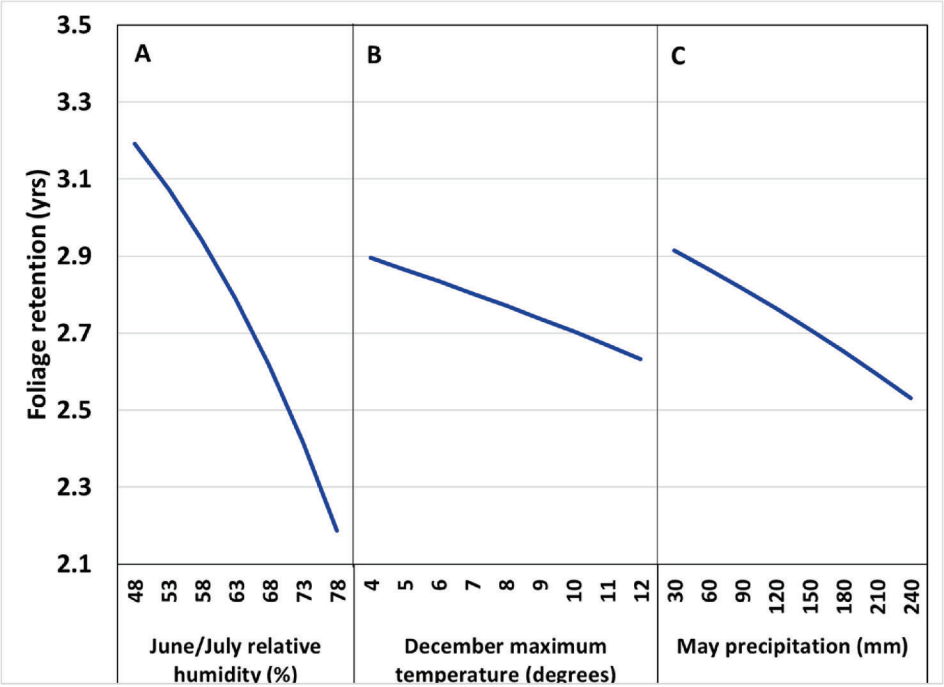

Fig. 3. Relationship between A) July relative humidity and foliage retention, B) December maximum temperature and foliage retention and C) May precipitation and foliage retention with all other variables in equation [2] held at their mean dataset levels.

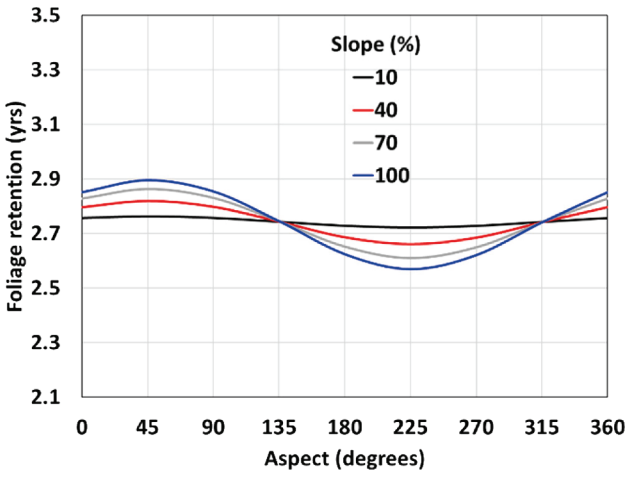

Fig. 4. Relationship between slope, aspect and foliage retention, with all other variables in equation [2] held at their mean dataset levels.

decreased with increasing December maximum temperature, varying approximately 0.25 years across the range of December temperatures in the dataset (Fig. 3b). Foliage retention also decreased with increasing May precipitation, varying approximately 0.4 years across the range of May precipitation in the dataset (Fig. 3c). Foliage retention was greatest on NE aspects and lowest on SW aspects, with the contrast increasing with increasing slope, and up to ~ 0.25 years on 70% slopes (Fig. 4). Foliage retentions were lower on ridgetops and greater in valleys or concave landforms, varying up to ~ 0.2 years on contrasting landforms (Fig. 5a), and increased with decreasing soil cation exchange capacity, ranging up to a 0.2 year difference (Fig. 5b). Lastly, foliage retention increased as elevations exceeded 400 m, all else being equal (Fig. 5c).

The mean square error of the equation [2] fit (0.222) was an improvement from the reported value of 0.25 for the best monthly model by Zhao et al. (2011) or the value of 0.26 reported using ordinary least squares regression by Latta et al. (2010, unpublished). No MSE values were reported for the Coop and Stone (2007) model.

When applied over a 400 m grid of systematic points across western Oregon and Washington, equation [2] predicts an increasing gradient of foliage retention from west to east, reflecting the current Swiss needle cast epidemic (Fig. 6). The lowest values of estimated foliage retention

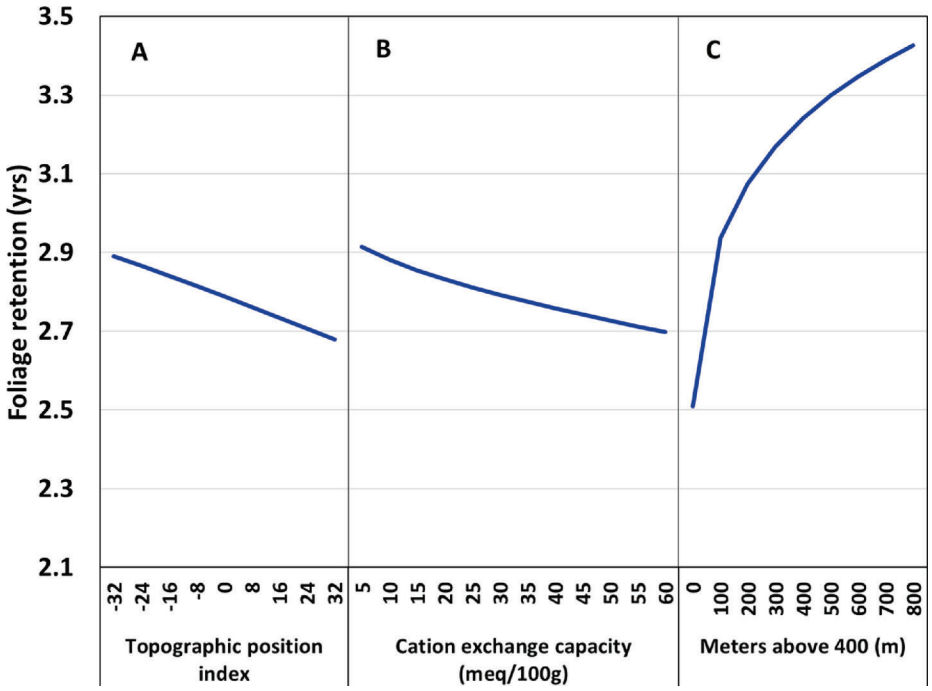

Fig. 5. Relationship between A) topographic position index (TPI) and foliage retention (positive TPI designates a convex landform; a negative TPI designates a concave landform), B) soil cation exchange capacity and foliage retention, and C) MA400 and foliage retention, with all other variables in equation [2] held at their mean dataset levels.

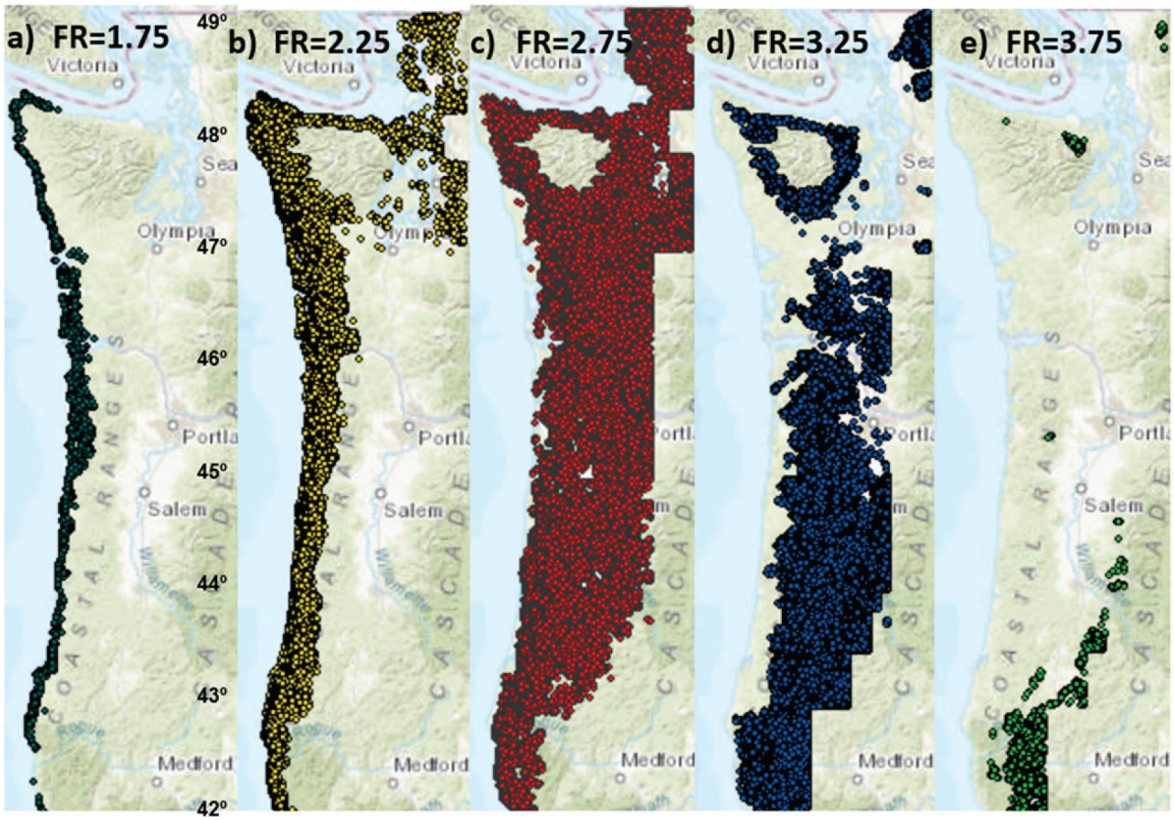

Fig. 6. Application of equation [2] to raster-extracted predictor variables on a 400 m grid of western Oregon and Washington. Categorized (a-e) by foliage retention class midpoint. Soils information was not available for Olympic National Park.

are predicted in the immediate vicinity of the Pacific Ocean and the highest values are considerably inland, while there is significant overlap of estimates throughout the Coast Range, a result of the complex topography and its influence on climate, and direct effects on other predictor variables. The effects of this complex topography on the variables that predict foliage retention is more apparent in the more localized estimates shown for the area near Newport, Oregon (Fig. 7).

4. Model validation

Model validation was conducted using the 824 observations removed from the available data for creation of the final modeling dataset. All predictor variables were calculated for each of the 824 validation observations, specific to the appropriate lagged year. Fig. 8 shows the calculated residuals from that effort, resulting in a final mean residual (observed-predicted) of 0.071 years and a mean absolute difference of 0.326 years. An additional cross-validation was performed by using equation [2] to predict the foliage retention from a random selection of one-third of the full dataset. This process, repeated 100 times, resulted in an average mean residual of 0.0328 years (standard deviation = 0.0142 years), and a maximum absolute value of 0.0681 years.

The validation dataset was also used to compare predictions between the current model and previous foliage retention model fits (Latta et al. 2010, Zhao et al. 2011), with residuals calculated separately for the pre-2010 datapoints (used for the previous models) and the post-2012 datapoints (used only for the current model). Mean residuals for the pre-2010 datapoints for the three models (current, Zhao et al. 2011, and Latta et al. 2010) were 0.095, −0.195, and 0.163 years respectively, and mean residuals for the post-2012 datapoints were −0.018, −1.005, and 0.070 years, respectively.

4.1. Growth impacts of foliage loss

Yield estimates from CIPSANON projections were combined with the proportional distribution of equation [2] foliage retention estimates by latitudinal class and zones representing distance from the Pacific Ocean (0–10 km, 10–20 km, 20–40 km, and 40–60 km) to produce a weighted average implied Scribner volume growth loss by location. Relative volume growth across different foliage retention classes was approximately equal for either cubic or Scribner volume (Fig. 9), though the relationship between relative Scribner volume production and foliage retention was noisier, due to the timing of production of different scaling diameters and log lengths, and inherent variation of volume calculation using a nominal scale. As Figs. 6-7 imply, estimated Scribner volume growth losses decreased with distance from the coast, and were relatively smaller in the southern zone of the study area (Fig. 10). In the zone nearest the Pacific Ocean, the largest average Scribner volume growth losses over a 50-year rotation (~23%) were predicted to be between 46 and 48°N latitude (Fig. 10). In the zone furthest from the Ocean (40–60 km), growth losses were estimated to be greatest in the northern-most latitudes, no doubt due to the climatic influence of Puget Sound.

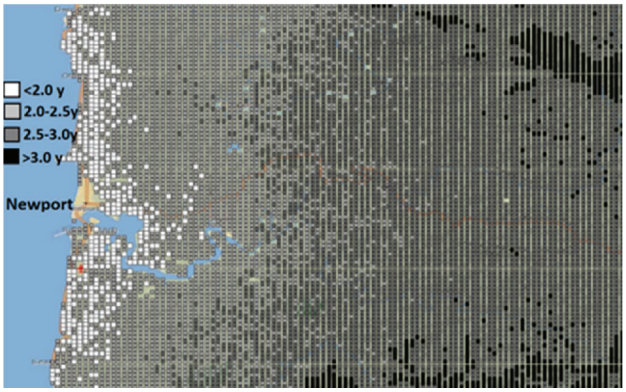

Fig. 7. Application of equation [2] to raster-extracted predictor variables on a 400 m grid of points up to 35 km east of Newport, Oregon and bounded by 44.5 and 44.8°N latitude.

5. Discussion

We found the lowest foliage retentions are predicted in a relatively narrow ribbon along the Pacific Ocean, with the greatest inland extent from Cascade Head, on the northern Oregon coast, to Grays Harbor in Washington. Also apparent is the limited extent of SNC symptoms along the southern Oregon coast, particularly south of Bandon, Oregon.

Douglas-fir foliage retention was found to be correlated with average June/July relative humidity, December maximum temperature, and May precipitation averaged for the periods of budbreak for the 2–4 yr old needle cohorts, a transformation of slope and aspect, a variable accounting for the number of meters above 400 m elevation, topographic position index, and soil cation exchange capacity.

Based on mean residuals, the current fit is an improvement relative to previous efforts, though the Latta et al. (2010) mean residuals were very similar. In contrast to the previous models, the data for the current model was based on a sampled four-year old branch (maximum foliage retention of 4.0 years), making comparisons among the models problematic for stands unaffected by foliar loss. If only accounting for sites with a foliage retention below 2.0 years, the mean absolute residual of the current model and the Latta et al. model is identical (-0.307 years) while the Zhao et al. model mean absolute residual is −0.55 years.

The equation [2] RMSE of ~ 0.47 years indicates that despite the improved fit relative to previous efforts, there is still a significant amount of unexplained variation in the estimate. This would seem to imply that the results from applying equation [2] to a single stand should be treated with caution. A more appropriate use of these results would be for application to estimate the foliage retention across many stands within an inventory to estimate the impacts of foliage loss over an entire ownership or landscape, such as is demonstrated in Figs. 6 and 7.

5.1. Weather variables and SNC

Based on the range of the response, average June and July relative humidity is the most influential of the predictor variables over its full range. Relative humidity and May precipitation are the variables representing spring moisture, previously identified as critical in the successful germination and development of the fungus on newly emerged foliage (Manter et al. 2005). Relative humidity is coarsely correlated with frequency of precipitation, mist, fog, and general maritime proximity, thus serving as an epidemiologically mechanistic variable. While May precipitation is important and significant, there is likely to be a greater contrast in June and July relative humidity between SNC-susceptible coastal sites and drier interior sites than is the case for late spring precipitation (Dye et al. 2020). The importance of winter temperature in the development of stomatal-plugging fruiting bodies (Manter et al. 2003), and represented in equation [2] by December maximum temperature, is notably less influential in predicting foliage retention than are the moisture surrogates (Fig. 3), but positive conditions for pseudothecial development is inconsequential if spores don't successfully germinate and colonize needles.

5.2. Landscape variables and SNC

Significant topographical features such as slope, aspect, elevation, and topographic position index are consistent with previous findings. Anecdotal observations have noted lower apparent foliage retentions on south slopes, and previous modeling efforts quantitatively identified W-SE slopes as having lower foliage retention (Rosso and Hansen 2003), in agreement with the minimization of foliage retention on a SW aspect shown in Fig. 4. This has been anecdotally reasoned to be due to greater

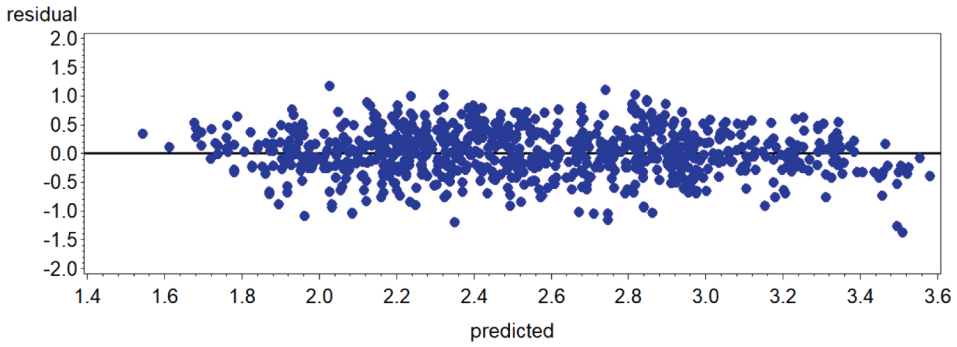

Fig. 8. Residuals vs. predictions from applying equation [2] to 824 validation observations not used in the original fitting.

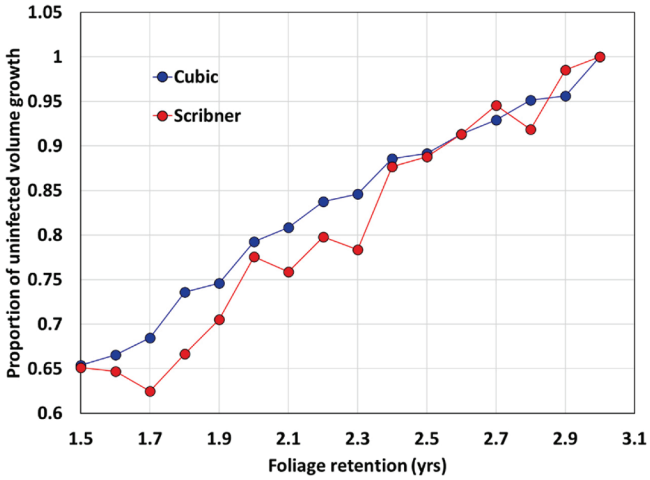

Fig. 9. Implied cubic and Scribner volume growth loss at age 50 years across a range of foliage retentions.

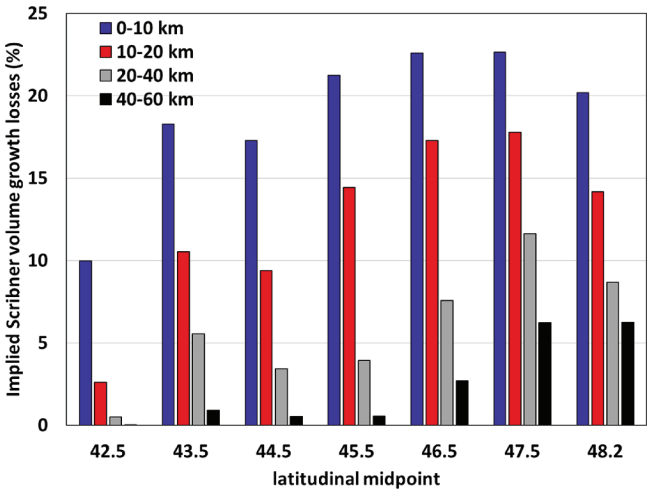

Fig. 10. Implied Scribner volume growth loss over a 50-year rotation of pure Douglas-fir by latitude class and distance from the Pacific Ocean.

winter temperatures relative to northern aspects. Comparisons between ClimateNA temperature estimates of different aspects at similar elevations on proximate topography with significant slopes suggests that ClimateNA temperature estimates don't differentiate by aspect. The parameter estimate of the topographic position index predictor variable, calculated from a 30 m DEM, implies lower foliage retention on convex topographies than concave topographies, which suggests a negative effect of exposed positions which may be warmer in winter, or perhaps a shallow soils effect. This contrasts with an earlier finding which found greater SNC symptoms in lower slope or valley positions, assumed due to the increased likelihood of fog or moisture, and the associated improvements in spore germination success (Rosso and Hansen 1999). Springtime moisture in the Rosso and Hansen (1999) work was represented by June precipitation only. Use of June/July relative humidity may better represent atmospheric moisture represented by fog, resulting in putting greater emphasis on other determinant aspects of topographic position vis-à-vis foliage retention.

Elevation is already represented in equation [2] through the bilinear interpolation and dynamic local elevational adjustment used to interpolate PRISM climate data within ClimateNA (Wang et al. 2016). The MA400 variable within equation [2], provides an additional elevation adjustment, based on both observation of regression residuals and evidence found in the pattern of foliage retention across an elevational gradient within sampled plots in the foothills of the Oregon Cascades (Ritóková et al. 2016, Ritóková et al. 2017). Furthermore, its addition greatly enhanced the precision of the predictions at higher elevations, reducing the MSE from 0.257 to 0.222.

Figs. 6 and 7 highlight the oft-noted relationship between SNC-influenced foliage retention and distance from the ocean. While this could be used as a predictor variable, our goal was to use predictors that had some epidemiological basis, and would be responsive to the variation in disease symptoms that can vary both temporally and geographically. Being a fixed effect that is collinear with elevation and numerous climate variables, distance from coast was not considered useful either for current or future predictions.

5.3. Soil variables and SNC

Another variable which may primarily differentiate between widely-infected coastal zones and interior areas with few signs of disease is soil cation exchange capacity. Whether the significance of soil cation exchange capacity is due to a causative effect of CEC on foliage retention or a correlation due to regional distribution of soil types is challenging to diagnose. One previous study with a more limited geographic sample also found a negative correlation between foliage retention and CEC based on plot soil sampling, but CEC in that dataset was also negatively correlated with distance from the ocean, and positively and negatively correlated with numerous other soil mineral elements (Mainwaring et al. 2014), such that any mechanistic explanation for inclusion of CEC quickly becomes complicated. Soils from sampled locations along the southern Oregon coast and in the more interior Cascades tend to have slightly different climates, greater foliage retentions, and lower average soil cation exchange capacities than the more northern coastal areas, as well as lower disease pressure. Inclusion of CEC within the model improved the MSE of equation [2] from 0.231 to 0.222 and improved the underestimation of foliage retention at low levels of CEC.

5.4. Other drivers of foliage retention

Our focus thus far considering SNC as the underlying cause of poor foliage retention mirrors many years of previous research (see references above), but other potential reasons for low or high needle retention must also be considered. For example, on a landscape scale, foliage retention in determinant-growth conifers naturally increases with decreasing site productivity and increasing elevation (Schoettle 1990, Reich et al. 1995, Xiao 2003). Additionally, short-term weather conditions, such as the 2021 heat dome event in western Washington and Oregon, or longer-term weather events, such as the persisting drought conditions in the Pacific Northwest (Iglesias et al. 2022), could also influence foliar retention regionally. These abiotic factors set the complicated baseline for the influence of foliage diseases and other biota which reduce needle retention (Shaw et al. 2014, Ritóková et al. 2021).

Consideration of non-SNC factors is also relevant as we were unable to include a direct metric of disease severity in this model, because disease severity measurements have not been taken as consistently or as widely ranging as foliar retention measurements. Unfortunately, needle retention as a proxy for direct fungal counts is not perfect, as the correlation between SNC-influenced needle retention and the percentage of stomatal occlusion by pseudothecia on retained foliage is weak over large areas (Ritóková et al. 2021). Even in areas where *N. gaeumanii* pseudothecia are abundant in late spring, such as in stands in western Oregon and Washington, correlation between needle retention and percent stomates occluded by fungal fruiting bodies has been inconsistent (Brooks et al. 2022), highlighting our current lack of knowledge about the dynamics of occlusion, SNC-influenced foliar loss, and other potential factors.

Without knowing all the causes of atypical foliar loss beyond SNC, it is unknown how appropriate the associations described in our equation [2] are, but the precision of the equation does not show geographic bias, suggesting that its use for estimating foliage retention across the region is robust. This estimation of foliage retention is significant regardless of its underlying cause, as needle retention below three years correlates well with reductions in Douglas-fir growth (Maguire et al. 2002). Therefore, the reality of foliage loss, and the associated diminishment of annual Douglas-fir increment, standing volume, and revenue, should make this model relevant to land managers throughout the region.

5.5. Growth impacts of foliage loss

A previous study has cited an average cubic volume growth loss of 23% for 10–30 year old Douglas-fir plantations in the northern Oregon Coast Range based on the relationship between cubic volume increment and foliage retention, and the average foliage retention across a plot network randomly chosen from among the population of 10–30 year old plantations (Maguire et al. 2002). The estimate here is not directly comparable, being based on a systematic sample of the landscape rather than a 77-plot sample, and based on an updated dataset that doesn't include the now-liquidated and species-converted stands that made up the most poorly performing stands of the original sample. Nonetheless, the average growth losses shown here are still lower than what has been previously estimated.

This current effort has included variables not used in the original foliage retention mapping work of Coop and Stone (2007), Latta et al. (2010), or Zhao et al. (2011). Still, additional clarification of environmental factors influencing SNC may be possible. Graphical analysis of the equation [2] residuals versus latitude using the entire dataset showed areas of local bias, with the most prominent being a gradient of underestimation to overestimation from about 45.1° N latitude to 45.5°N latitude (Fig. 11). The Oregon coast has two broad river basins in that area: the Nestucca drainage, forming a SW-NE river valley at the south end of the gradient, and the Tillamook basin, a broad drainage basin of five rivers at the northern end of this gradient. It is assumed that the foliage retention overestimate may be related to the topographic-influenced accessibility of marine air further into the Coast Range through the Tillamook basin and the Nestucca drainage, otherwise unaccounted for by ClimateNA variable estimates, and that the underestimate at the south end of the gradient may be related to the presence of the 500-plus meter Cascade Head and the Nestucca drainage's northeast-ward course serving to direct marine air to the NE. Variables were produced by calculating near-coast average elevations west of specific sample points, weighted (or not) by distance from the coast in an attempt to explain some of the local variation seen in Fig. 11. Some of these efforts were statistically, though not quantitatively significant, and had no discernable effect on the local bias in foliage retention apparent in Fig. 11. Given the fixed topography, it might be possible to produce descriptive topographic variables for use within the model using an RSAGA module or GIS spatial analysis that could be related to windflow or some other influential factor.

6. Conclusions

This new model represents an improvement to earlier published foliage retention models, both in its precision and the geographic range of the data used in its construction. Furthermore, the results of this analysis can be put into immediate practical use. The use of spatially explicit foliage retentions in populating growth model input for compilation or simulation of infected stands can be easily accomplished through an R interface, directing the extraction of equation [2] predictor variables from separate rasters, based on an input latitude and longitude. In its dependence on broad scale climate and soils data, which themselves are interpolated from point data from a dataset of limited size, the model can provide unbiased estimates of foliage retention which are accurate, on average, over a large region. Nonetheless, the relatively large MSE of equation [2] underscores the imperfection of single point estimates.

CRediT authorship contribution statement

Douglas B. Mainwaring: Methodology, Writing – original draft. **Gabriela Ritóková:** Writing – review & editing. **David C. Shaw:**

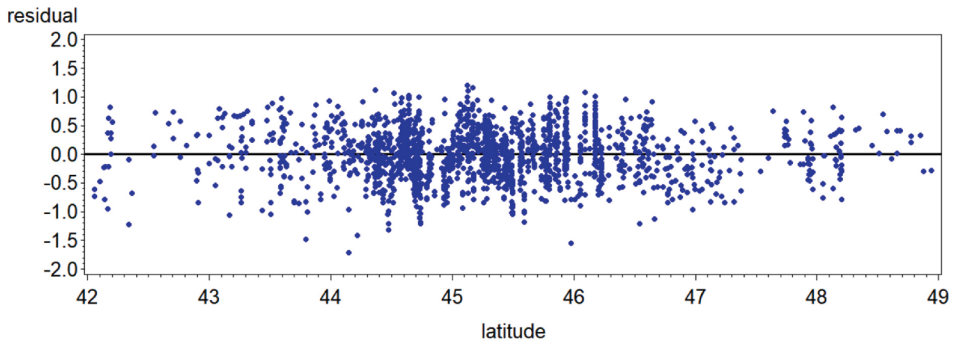

Fig. 11. Plot of regression residuals versus latitude from fitting equation [2] with the full dataset.

Writing – review & editing. **Rachel K. Brooks:** Writing – review & editing. **Daniel W. Omdal:** Writing – review & editing.

Declaration of Competing Interest

The authors declare that they have no known competing financial interests or personal relationships that could have appeared to influence the work reported in this paper.

Data availability

The data that has been used is confidential.

References

Balster, N.J., Marshall, J.D., 2000. Decreased needle longevity of fertilized Douglas-fir and grand fir in the northern Rockies. Tree Physiology. 20, 1191–1197.

Brenning, A., Bangs, D., Becker, M., Schratz, P., Polakowski, F., 2018. SAGA Geoprocessing and terrain analysis. R. Package Version 1 (3).

Brooks, R., Omdal, D. 2021. 2021 SNC ground sampling in Washington. P. 12-14 in Swiss Needle Cast Cooperative annual report, Ritóková. G. (ed.). College of Forestry, Oregon State Univ., Corvallis, OR.

Brooks, R., Omdal, D., Davis, I., Kohler, G., Hof, J., Kimbrel, M., Okasaki, C., 2022. Western Washington Swiss needle cast aerial and ground survey, 2021–2022. Washington State Department of Natural Resources.

Bruce, D., 1981. Consistent height-growth and growth-rate estimates for remeasured plots. For. Sci. 27, 711–725.

Coop, L., Stone, J. 2007. P. 15-21 in Swiss Needle Cast Cooperative annual report, Shaw, D. (ed.). College of Forestry, Oregon State Univ., Corvallis, OR.

Dye, A.W., Rastogi, B., Clemesha, R.E.S., Kim, J.B., Samelson, R.M., Still, C.J., Williams, A.P., 2020. Spatial patterns and trends of summertime low cloudiness for the Pacific Northwest, 1996–2017. Geophysical Research Letters e2020GL088121.

Freeman, F., 2002. Swiss needle cast monitoring in the Oregon Cascades. P. 11-14 in Swiss Needle Cast Cooperative annual report, Filip. G. (ed.). College of Forestry, Oregon State Univ., Corvallis, OR.

Gower, S.T., Vogt, K.A., Grier, C.C., 1992. Carbon dynamics of Rocky Mountain Douglas-fir: influence of water and nutrient availability. Ecol. Monogr. 62, 43–65.

Hansen, E.M., Stone, J.K., Capitano, B.R., Rosso, P., Sutton, W., Winton, L., Kanaskie, A., McWilliams, M.G., 2000. Incidence and impact of Swiss needle cast in forest plantations of Douglas-fir in coastal Oregon. Plant disease 84, 773–778.

Herpin-Saunier, N.Y., Sambaraju, K.R., Yin, X., Feau, N., Zeglen, S., Ritóková, G., Omdal, D., Côté, C., Hamelin, R.C., 2022. Genetic lineage distribution modelling to predict epidemics of a conifer disease. Front. Forests Global Change. https://doi.org/10.3389/ffgc.2021.756678.

Iglesias, V., Travis, W.R., Balch, J.K., 2022. Recent droughts in the United States are among the fastest-developing of the last seven decades. Weather Climate Extremes. 37, 100491.

Latta, G., Adams, D., Shaw, D., 2010. Mapping western Oregon Douglas-fir foliage retention with a simultaneous autoregressive model. https://sncc.forestry.oregonstate.edu/models.

Maguire, D.A., Kanaskie, A., Voelker, W., Johnson, R., Johnson, G., 2002. Growth of young Douglas-fir plantations across a gradient in Swiss needle cast severity. Western J. Appl. Forest. 17, 86–95.

Maguire, D.A., Mainwaring, D.B., Kanaskie, A., 2011. Ten-year growth and mortality in young Douglas-fir stands experiencing a range in Swiss needle cast severity. Can. J. Forest Res. 41, 2064–2076.

Mainwaring , D. , Maguire , D. , 2008 . Trends in foliage retention on the growth impact and pre-commerical thinning plots. P. 21-24 in Swiss Needle Cast Cooperative annual report, Shaw, D. and Woolley, T. (Eds). College of Forestry, Oregon State Univ, Corvallis, OR.

Mainwaring, D.B., and Maguire, D.A. 2020. The effects of Swiss needle cast on stem taper and its incorporation into CIPSANON/ORGANON. CIPS Technical Report #18. Internal Report. 7 pp.

Mainwaring D., Carr, J., Maguire, D., 2004. Menasha silvicultural trials: Response of SNC-impacted Douglas-fir to intensive silvicultural treatments. P. 75-79 in Swiss Needle Cast Cooperative annual report, Mainwaring, D. (ed.). College of Forestry, Oregon State Univ., Corvallis, OR.

Mainwaring D., Maguire, D., Kanaskie, A., and Brandt, J. 2007. Douglas-fir Growth Response to Commercial Thinning in the Presence of Swiss Needle Cast in North Coastal Oregon. P. 22-34 in Swiss Needle Cast Cooperative annual report, Shaw, D. (ed.). College of Forestry, Oregon State Univ., Corvallis, OR.

Mainwaring, D.B., Hann, D.H., Maguire. D.A., and Zhao, J. 2020. Effect of Swiss needle cast infections upon diameter and height increment of Douglas-fir trees. CIPS Technical Report #7. Internal Report. 10 pp.

Mainwaring, D.B., Maguire, D.A., Perakis, S.S., 2014. Three-year growth response of young Douglas-fir to nitrogen, calcium, phosphorus, and blended fertilizers in Oregon and Washington. Forest Ecol. Manage. 327, 178–188.

Manter, D.K., Bond, B.J., Kavanagh, K.L., Rosso, P.H., Filip, G.M., 2000. Pseudothecia of Swiss needle cast fungus, Phaeocryptopus gaeumannii, physically block stomata of Douglas-fir, reducing CO_2. New Phytologist. 2000, 481–491.

Manter, D.K., Winton, L.M., Filip, G.M., Stone, J.K., 2003. Assessment of Swiss needle cast disease: temporal and spatial investigations of fungal colonization and symptom severity. J. Phytopathology. 151, 344–351.

Manter, D.K., Reeser, P.W., Stone, J.K., 2005. A climate-based model for predicting geographic variation in Swiss needle cast severity in the Oregon Coast Range. Phytopathology 95 (11), 1256–1265.

R Core Team, 2021. 'R: A Language and Environment for Statistical Computing'. R Foundation for Statistical Computing. Available at: https://www.r-project.org/.

Reich, P.B., Koike, T., Gower, S.T., Schoettle, A.W., 1995. Causes and consequences of variation in conifer leaf life-span. In Ecophysiology of coniferous forests. Edited by W.K. Smith and T.M. Hinckley. Academic Press, New York. pp. 225–254.

Ritóková, G. and Shaw, D., 2020. SNC Transect plots in the Oregon Cascades foothills. P. 45-46 in Swiss Needle Cast Cooperative annual report, Ritóková, G. and Shaw, D. (eds.). College of Forestry, Oregon State Univ., Corvallis, OR.

Ritóková, G., Shaw, D. Mainwaring D., Maguire, D., Marshall, B., 2017. SNC Transect plots in the Oregon Cascades foothills. P. 45-50 in Swiss Needle Cast Cooperative annual report, Ritóková, G. and Shaw, D. (eds.). College of Forestry, Oregon State Univ., Corvallis, OR.

Ritóková, G., Shaw, D.C., Filip, G., Kanaskie, A., Browning, J., Norlander, D., 2016. Swiss Needle Cast in Western Oregon Douglas-Fir Plantations: 20-Year Monitoring Results. Forests 7, 155.

Ritóková, G., Mainwaring, D.B., Shaw, D.C., Lan, Y.-H., 2021. Douglas-fir foliage retention dynamics across a gradient of Swiss needle cast in Oregon and Washington. Can. J. Forest Res. 51, 573–582.

Rosso, P.H., Hansen, E.M. 1999. Swiss needle cast risk analysis and modeling. P. 69-76 in Swiss Needle Cast Cooperative annual report, Ritóková, G. and Shaw, D. (eds.). College of Forestry, Oregon State Univ., Corvallis, OR.

Rosso, P.H., Hansen, E.M., 2003. Predicting Swiss needle cast disease distribution and severity in young Douglas-fir plantations in coastal Oregon. Phytopathology 93, 790–798.

Schoettle, A.W., 1990. The interaction between leaf longevity, shoot growth, and foliar biomass per shoot in *Pinus contorta* at two elevations. Tree Physiol. 7, 209–214. https://doi.org/10.1093/treephys/7.1-2-3-4.209. PMID:14972918.

Shaw, D., Woolley, T., 2009. Needle Retention Estimates of the southern Oregon Coast and southwest Washington P. 33-36 in Swiss Needle Cast Cooperative annual report, Shaw, D. and Woolley, T. (eds.). College of Forestry, Oregon State Univ., Corvallis, OR.

Shaw, D.C., Filip, G.M., Kanaskie, A., Maguire, D.A., Littke, W., 2011. Managing an epidemic of Swiss needle cast in the Douglas-fir region of Oregon: The Swiss Needle Cast Cooperative. J. Forestry 109, 109–119.

Shaw, D.C., Woolley, T., Kanaskie, A., 2014. Vertical foliage retention in Douglas-fir across environmental gradients of the western Oregon Coast Range influenced by Swiss Needle Cast. Northwest Sci. 88, 23–32.

Shaw, D.C., Ritóková, G., Lan, Y.-H., Mainwaring, D.B., Russo, A., Comeleo, R.L., Navarro, S., Norlander, D., Smith, B., 2021. Persistence of the Swiss Needle Cast Outbreak in Oregon Coastal Douglas-fir, and New Insights from Research and Monitoring. J. Forest. 119, 407–421.

Stage, A.R., 1976. An expression for the effect of aspect, slope, and habitat type on tree growth. For. Sci. 22, 457–460.

Stage, A.R., Salas, C., 2007. Interactions of elevation, aspect, and slope in models of forest species composition and productivity. Forest Science 53, 486–492.

Wang, T., Hamann, A., Spittlehouse, D., Carroll, C., 2016. Locally Downscaled and Spatially Customizable Climate Data for Historical and Future Periods for North America. PLoS ONE 11 (6), e0156720.

Xiao, Y., 2003. Variation in needle longevity of Pinus tabulaeformis forest at different geographic scales. Tree Physiol. 23, 463–471. https://doi.org/10.1093/treephys/23.7.463. PMID:12670800.

Zhao, J., Mainwaring, D.B., Maguire, D.A., Kanaskie, A., 2011. Regional and annual trends in Douglas-fir foliage retention: Correlations with climatic variables. For. Ecol. Man. 262, 1872–1886.

List of Refereed Publications

Disease Distribution, Severity and Epidemiology

Agne, MC, Beedlow PA, Shaw DC, Woodruff DR, Lee EH, Cline S, Comeleo RL. 2018. Interactions of predominant insects and diseases with climate change in Douglas-fir forests of western Oregon and Washington, U.S.A.. Forest Ecology and Management. 409:317-332.

Hansen, E. M., Stone, J. K., Capitano, B. R., Rosso, P., Sutton, W., Winton, L., Kanaskie, A. and M. G. McWilliams. 2000. Incidence and impact of Swiss needle cast in forest plantations of Douglas-fir in coastal Oregon. Plant Disease. 84: 773-779.

Hennon, P.E., Frankel, S.J., Woods, A.J., Worrall, J.J., Ramsfield, T.D., Zambino, P.J., Shaw, D.C., Ritóková, G., Warwell, M.V., Norlander, D. and Mulvey, R.L., 2021. Applications of a conceptual framework to assess climate controls of forest tree diseases. Forest Pathology, 51(6), p.e12719.

Lan Y-H, Shaw D.C., Beedlow P.A., Lee E.H., Waschmann R.S.. 2019. Severity of Swiss needle cast in young and mature Douglas-fir forests in western Oregon, USA. Forest Ecology and Management. 442:79-95.

Manter, D. K., Reeser, P. W., and J. K. Stone. 2005. A climate-based model for predicting geographic variation in Swiss needle cast severity in the Oregon coast range. Phytopathology. 95: 1256-1265.

Ritóková, G, Shaw DC, Filip GM, Kanaskie A, Browning J, Norlander D. 2016. Swiss Needle Cast in Western Oregon Douglas-Fir Plantations: 20-Year Monitoring Results. Forests. 7(155)

Ritóková, G, Mainwaring, D.B., Shaw D.C., Lan, Y-H. 2020. Douglas-fir foliage retention dynamics across a gradient of Swiss needle cast in coastal Oregon and Washington. Canadian Journal of Forest Research. https://doi.org/10.1139/cjfr-2020-0318

Rosso, P. H. and E. M. Hansen. 2003. Predicting Swiss needle cast disease distribution and severity in young Douglas-fir plantations in coastal Oregon. Phytopathology. 93: 790-798.

Shaw D.C., Ritóková, G, Lan, Y-H, Mainwaring, D.B., Russo, A., Comeleo, R., Navaro, S., Norlander, D., Smith, B. 2021. Persistence of the Swiss Needle Cast Outbreak in Oregon Coastal Douglas-fir, and New Insights from Research and Monitoring. Journal of Forestry.

Stone, J. K., Hood, I. A., Watt, M. S. and J. L. Kerrigan. 2007. Distribution of Swiss needle cast in New Zealand in relation to winter temperature. Australasian Plant Pathology. 36: 445-454.

Stone, J. K., Capitano, B. R. and J. L. Kerrigan. 2008. The histopathology of *Phaeocryptopus gaeumannii* on Douglas-fir needles. Mycologia. 100: 431-444.

Stone, J. K., Coop, L. B. and D. K. Manter. 2008. Predicting the effects of climate change on Swiss needle cast disease severity in Pacific Northwest forests. Canadian Journal of Plant Pathology. 30: 169-176.

Watt, M. S., Stone, J. K., Hood, I. A. and D. J. Palmer. 2010. Predicting the severity of Swiss needle cast on Douglas-fir under current and future climate in New Zealand. Forest Ecology and Management (*in press*).

Forest Protection Issues

Kelsey, R. G. and D. K. Manter. 2004. Effect of Swiss needle cast on Douglas-fir stem ethanol and monoterpene concentrations, oleoresin flow, and host selection by the Douglas-fir beetle. Forest Ecology and Management. 190: 241-253.

Shaw, D. C., Filip, G. M., Kanaskie, A., Maguire, D. A. and W. Littke. 2011. Managing an epidemic of Swiss needle cast in the Douglas-fir region of Oregon: The Swiss Needle Cast Cooperative. Journal of Forestry (*in press*).

Genetic Resistance/Tolerance in Douglas-fir

Jayawickrama, K.J.S., D. Shaw, and T.Z. Ye. 2012. Genetic Selection in Coastal Douglas-fir for tolerance to Swiss Needle Cast Disease. Proceedings of the fourth international workshop on the genetics of host-parasite interactions in forestry: Disease and insect resistance in forest trees. Gen. Tech. Rep. PSW-GTR-240. Albany, CA: Pacific Southwest Research Station, Forest Service, U.S. Department of Agriculture. 372 p.

Johnson, G. R. 2002. Genetic variation in tolerance of Douglas-fir to Swiss needle cast as assessed by symptom expression. Silvae Genetica. 51: 80-86.

Kastner, W., Dutton, S. and D. Roche. 2001. Effects of Swiss needle cast on three Douglas-fir seed sources on a low-elevation site in the northern Oregon Coast Range: Results after five growing seasons. Western Journal of Applied Forestry. 16 (1): 31-34.

Temel, F., Johnson, G. R. and J. K. Stone. 2004. The relationship between Swiss needle cast symptom severity and level of *Phaeocryptopus gaeumannii* colonization in coastal Douglas-fir (*Pseudotsuga menziesii var. menziesii*). Forest Pathology. 34: 383-394.

Temel, F., Johnson, G. R. and W. T. Adams. 2005. Early genetic testing of coastal Douglas-fir for Swiss needle cast tolerance. Canadian Journal of Forest Research. 35: 521-529.

Wilhelmi, N.P., Shaw D.C., Harrington C.A., St. Clair J.B., Ganio L.M. 2017. Climate of seed source affects susceptibility of coastal Douglas-fir to foliage diseases. Ecosphere. 8(12):e02011.

Genetics of Nothophaeocryptopus gaeumannii

Bennett P, Hood P.I, Stone J.K.. 2018. The genetic structure of populations of the Douglas-fir Swiss needle cast fungus *Nothophaeocryptopus gaeumannii* in New Zealand. Phytopathology. 109:446-455.

Bennett P, Stone J.K.. 2019. Environmental variables associated with *Nothophaeocryptopus gaeumannii* population structure and Swiss needle cast severity in Western Oregon and Washington. Ecology and Evolution. 9(19):11379-11394.

Herpin-Saunier, N.Y., Sambaraju, K.R., Yin, X., Feau, N., Zeglen, S., Ritokova, G., Omdal, D., Côté, C. and Hamelin, R.C.. 2022. Genetic lineage distribution modeling to predict epidemics of a conifer disease. Frontiers in Forests and Global Change. 4:229-243.

Winton, L. M., Hansen, E. M. and J. K. Stone. 2006. Population structure suggests reproductively isolated lineages of *Phaeocryptopus gaeumannii*. Mycologia. 98 (5): 781-791.

Winton. L. M., Stone, J. K. and E. M. Hansen. 2007. The systematic position of *Phaeocryptopus gaeumannii*. Mycologia. 99: 240-252.

Hydrology

Bladon KD, Bywater-Reyes S, LeBoldus JM, Keriö S, Segura C, Ritóková G, Shaw D.C.. 2019. Increased streamflow in catchments affected by a forest disease epidemic. Science of The Total Environment. 691:112-123.

Mensuration and growth effects

Lee, E.H., Beedlow P.A., Waschmann R.S., Tingey D.T., Cline S., Bollman M., Wickham C., Carlile C. 2017. Regional patterns of increasing Swiss needle cast impacts on Douglas-fir growth with warming temperatures. Ecology and Evolution. 7(24):11167–11196.

Maguire D. A., Kanaskie, A., Voelker, W., Johnson, R. and G. Johnson. 2002. Growth of young Douglas-fir plantations across a gradient in Swiss needle cast severity. Western Journal of Applied Forestry. 17: 86-95.

Maguire, D. A. and A. Kanaskie. 2002. The ratio of live crown length to sapwood area as a measure of crown sparseness. Forest Science. 48: 93-100.

Maguire, D. A., Mainwaring, D. B. and Kanaskie A. 2011. Ten-year growth and mortality in young Douglas-fir stands experiencing a range in Swiss needle cast severity. Can. J. For. Res. 41: 2064-2076.

Mainwaring, D. B., Ritóková, G., Shaw, D. C., Brooks, R. K., and Omdal, D. W. 2023. Site-level estimates of Douglas-fir foliage retention from climate, soil, and topographic variables. Forest Ecology and Management. 537:120930.

Weiskittel, A. R., Garber, S. M., Johnson, G. P., Maguire, D. A. and R.A. Monserud. 2007. Annualized diameter and height growth equations for Pacific Northwest plantation-grown Douglas-fir, western hemlock, and red alder. Forest Ecology and Management. 250: 266-278.

Weiskittel, A. R., Maguire, D. A., Garber, S. M. and A. Kanaskie. 2006. Influence of Swiss needle cast on foliage age class structure and vertical distribution in Douglas-fir plantations of north coastal Oregon. Canadian Journal of Forest Research. 36: 1497-1508.

Weiskittel, A. R., Maguire, D. A. and R. A. Monserud. 2007. Modeling crown structural responses to competing vegetation control, thinning, fertilization, and Swiss needle cast in coastal Douglas-fir of the Pacific Northwest, USA. Forest Ecology and Management. 245: 96-109.

Weiskittel, A. R., Maguire, D. A. and R. A. Monserud. 2007. Response of branch growth and mortality to silvicultural treatments in coastal Douglas-fir plantations: Implications for predicting tree growth. Forest Ecology and Management. 251: 182-194.

Weiskittel, A. R. and D. A. Maguire. 2007. Response of Douglas-fir leaf area index and litterfall dynamics to Swiss needle cast in north coastal Oregon, USA. Annals of Forest Science. 64: 121-132.

Weiskittel, A. R. and D. A. Maguire. 2006. Branch surface area and its vertical distribution in coastal Douglas-fir. Trees. 20: 657-667.

Weiskittel, A. R., Temesgen, H., Wilson, D. S. and D. A. Maguire. 2008. Sources of within and between-stand variability in specific leaf area of three ecologically distinct conifer species. Annals of Forest Science. 65: 103-112.

Zhao, J., Maguire, D. A., Mainwaring, D. B., Kanaskie, A. 2012. Climatic influences on needle cohort survival mediated by Swiss needle cast in coastal Douglas-fir. Trees 26: 1361-1371

Zhao, J., Mainwaring, D. B., Maguire, D. A., Kanaskie, A. 2011. Regional and annual trends in Douglas-fir foliage retention: Correlations with climatic variables. For. Ecol. And Management 262: 1872-1886

Zhao, J, Maguire DA, Mainwaring DB, Kanaskie A. 2015. The effect of within-stand variation in Swiss needle cast intensity on Douglas-fir stand dynamics. Forest Ecology and Management. 347:75-82.

Zhao, J., Maguire, D. A., Mainwaring, D. B., Wehage, J., Kanaskie, A. 2013. Thinning Mixed Species Stands of Douglas-Fir and Western Hemlcok in the Presence of Swiss Needle Cast: Guidelines Based on Relative Basal Area Growth of Individual Trees. For. Sci. 60 (1): 191-199.

Nutrition and soil interactions

El-Hajj, Z., Kavanagh, K., Rose, C., and Z. Kanaan-Atallah. 2004. Nitrogen and carbon dynamics of a foliar biotrophic fungal parasite in fertilized Douglas-fir. New Phytologist. 163: 139-147.

Lan Y-H, Shaw D.C., Ritóková G, Hatten J. 2019. Associations between Swiss Needle Cast Severity and Foliar Nutrients in Young-Growth Douglas-Fir in Coastal Western Oregon and Southwest Washington, USA. For. Sci. 65(5):537-542.

Mulvey, R.L., Shaw, D.C., Maguire, D.A. 2013. Fertilization impacts on Swiss needle cast disease severity in Western Oregon. Forest Ecology and Management 287: 147-158.

Perakis, S. S., Maguire, D. A., Bullen, T. D., Cromack, K., Waring, R. H. and J. R. Boyle. 2005. Coupled nitrogen and calcium cycles in forests of the Oregon Coast Range. Ecosystems. 8: 1-12.

Waring, R. H., Boyle, J., Cromack, K. Jr., Maguire, D. and A. Kanaskie. 2000. Researchers offer new insights into Swiss needle cast. Western Forester. 45 (6): 10-11.

Pathology and physiological host effects

Bennett, P., Stone, J. 2016. Assessments of Population Structure, Diversity, and Phylogeography of the Swiss Needle Cast Fungus (*Phaeocryptopus gaeumannii*) in the U.S. Pacific Northwest. Forests: 7, 14.

Black, B. A., Shaw, D. C. and J. K. Stone. 2010. Impacts of Swiss needle cast on overstory Douglas-fir forests of western Oregon Coast Range. Forest Ecology and Management. 259: 1673-1680.

Gervers, K. A., Thomas, D. C., Roy, B. A., Spatafora, J. W. and Busby, P. E. 2022. Crown closure affects endophytic leaf mycobiome compositional dynamics over time in *Pseudotsuga menziesii* var. *menziesii*. Fungal Ecology. 57–58:101155.

Lee, E.H., Beedlow, P.A., Waschmann, R.S., Cline, S., Bollman, M., Wickham, C. and Testa, N., 2021. Tree-ring history of Swiss needle cast impact on Douglas-fir growth in Western Oregon: correlations with climatic variables. J Plant Sci Phytopathol. 5:076-087.

Lee, E.H., Beedlow, P.A., Brooks, J.R., Tingey, D.T., Wickham, C. and Rugh, W., 2022. Physiological responses of Douglas-fir to climate and forest disturbances as detected by cellulosic carbon and oxygen isotope ratios. Tree Physiology, 42(1):5-25.

Lee, H.E., Beedlow, P.A., Waschamnn, R.S., Burdick, C.A., Shaw, D.C. 2013. Tree-ring analysis of the fungal disease Swiss needle cast in western Oregon coastal forests. Can Journal of For. 43(8):677-690.

Manter, D. K., Bond, B. J., Kavanagh, K. L., Rosso, P. H. and G. M. Filip. 2000. Pseudothecia of Swiss needle cast fungus, *Phaeocryptopus gaeumannii,* physically block stomata of Douglas-fir, reducing CO_2 assimilation. New Phytologist. 148 (3): 481-491.

Manter, D. K. 2002. Energy dissipation and photoinhibition in Douglas-fir needles with a fungal-mediated reduction in photosynthetic rates. Phytopathology. 150: 674-679.

Manter, D. K., Bond, B. J., Kavanagh, K. L., Stone, J. K. and G. M. Filip. 2003. Modeling the impacts of the foliar pathogen, *Phaeocryptopus gaeumannii*, on Douglas-fir physiology: net canopy carbon assimilation, needle abscission and growth. Ecological Modeling. 164: 211-226.

Manter, D. K. and Kavanagh, K. L. 2003. Stomatal regulation in Douglas-fir following a fungal-mediated chronic reduction in leaf area. Trees. 17: 485-491.

Manter, D. K., Kelsey, R. G., and J. K. Stone. 2001. Quantification of *Phaeocryptopus gaeumannii* colonization in Douglas-fir needles by ergosterol analysis. Forest Pathology. 31: 229-240.

Manter, D. K., Winton, L. M., Filip, G. M. and J. K. Stone. 2003. Assessment of Swiss needle cast disease: temporal and spatial investigations of fungal colonization and symptom severity. Phytopathology. 151: 344-351.

Saffell, B.J., Meinzer, R.C., Voelker, S.L., Shaw, D.C., Brooks, R.J., Lachenbruch, B, McKay, J. 2014. Tree-ring stable isotopes record the impact of a foliar fungal pathogen on CO_2 assimilation and growth in Douglas-fir. Plant, Cell & Environment. doi: 10.1111/pce.12256

Winton, L. M., Manter, D. K., Stone, J. K. and E. M. Hansen. 2003. Comparison of biochemical, molecular and visual methods to quantify *Phaeocryptopus gaeumannii* in Douglas-fir foliage. Phytopathology. 93: 121-126.

Winton, L. M., Stone, J. K., Watrud, L. S. and E. M. Hansen. 2002. Simultaneous one-tube quantification of host and pathogen DNA with real-time polymerase chain reaction. Phytopathology. 92: 112-116.

Winton, L. M., Stone, J. K. and E. M. Hansen. 2007. Polymorphic microsatellite markers for the Douglas-fir pathogen *Phaeocryptopus gaeumannii*, causal agent of Swiss needle cast disease. Molecular Ecology. 7: 1125-1128.

Silviculture and Control

Filip, G., Kanaskie, A., Kavanagh, K., Johnson, G., Johnson, R. and D. Maguire. 2000. Research Contribution 30, Forest Research Laboratory, College of Forestry, Oregon State University, Corvallis, Oregon.

Mainwaring, D. B., Maguire, D. A., Kanaskie, A. and J. Brandt. 2005. Growth responses to commercial thinning in Douglas-fir stands with varying intensity of Swiss needle cast. Canadian Journal of Forest Research. 35: 2394-2402.

Stone, J. K., Reeser, P. W. and A. Kanaskie. 2007. Fungicidal suppression of Swiss needle cast and pathogen reinvasion in a 20-year-old Douglas-fir stand. Western Journal of Applied Forestry. 22: 248-252.

Wood Quality

Grotta, A. T., Leichti, R. J., Gartner, B. L. and G. R. Johnson. 2004. Effect of growth ring orientation and placement of earlywood and latewood on MOE and MOR of very-small clear Douglas-fir beams. Wood and Fiber Science. 37: 207-212.

Johnson, G. R., Gartner, B. L., Maguire, D. and A. Kanaskie. 2003. Influence of Bravo fungicide applications on wood density and moisture content of Swiss needle cast affected Douglas-fir trees. Forest Ecology and Management. 186: 339-348.

Johnson, G. R., Grotta, A. T., Gartner, B. L. and G. Downes. 2005. Impact of the foliar pathogen Swiss needle cast on wood quality of Douglas-fir. Canadian Journal of Forest Research. 35: 331-339.

Lachenbruch, B., Johnson, G.R. 2020. Different radial growth rate effects on outerwood properties of coastal Douglas-fir in healthy trees vs. trees impacted by Swiss Needle Cast. Canadian Journal of Forest Research. https://doi.org/10.1139/cjfr-2020-0199